Hindawi
Applied and Environmental Soil Science
Volume 2023, Article ID 8475504, 23 pages
https://doi.org/10.1155/2023/8475504

Review Article

State-of-the-Art Graphene Synthesis Methods and Environmental Concerns

Kaamil Edward[1], **Kabir Mamun**[1], **Sumesh Narayan**[1], **Mansour Assaf**[1], **David Rohindra**[2] and **Upaka Rathnayake**[3,4]

[1]*School of Information Technology Engineering Mathematics and Physics (STEMP), The University of the South Pacific, Suva, Fiji*
[2]*School of Biological and Chemical Sciences, Faculty of Science Technology and Environment, The University of the South Pacific, Suva, Fiji*
[3]*Department of Civil Engineering, Faculty of Engineering, Sri Lanka Institute of Information Technology, Malabe, Sri Lanka*
[4]*Department of Civil Engineering and Construction, Faculty of Engineering and Design, Atlantic Technological University, Sligo, Ireland*

Correspondence should be addressed to Upaka Rathnayake; upaka.r@sliit.lk

Received 1 July 2022; Revised 9 November 2022; Accepted 11 January 2023; Published 2 February 2023

Academic Editor: Mahmoud Nasr

Graphene, a 2D sp^2 hybridized carbon sheet consisting of a honeycomb network, is the building block of graphite. Since its discovery in 2004, graphene's exceptional electronic and mechanical properties have peaked interest in various applications. However, the inability to mass produce high-quality graphene affordably currently limits the practical application of the material. Researchers are continuously working on advancing graphene synthesis methods to alleviate these limitations. Therefore, this review looks at the overview of established graphene synthesis methods and characterization techniques, and then highlights an in-depth review of graphene production through flash joule heating. The environmental concerns related to graphene synthesis are also presented in this review paper.

1. Introduction

Since graphene was first isolated in 2004, research on production methods and applications have increasingly progressed due to its unique properties which suggest the imminent transformation in the materials used in electronics, composites, energy, and anticorrosive coats. With demand for graphene and graphene-based materials growing (an estimated USD 170 million in global markets by 2022), there is a need to synthesize it at an industrial capacity. Existing manufacturing methods are not fully capable of producing reliable and cost-effective graphene to meet industrial applications; hence, the implementation of graphene has been limited [1]. However, the waste can be converted into high-quality turbostratic graphene using the flash joule heating (FJH) process. The FJH method shows the immense capability of being a scalable and cost-effective synthesis process because of the compatibility of the process with various carbon precursors without the need for pretreating with chemicals, buffer gases, substrates, or washing of graphene.

Joule heating approach has been previously investigated for the synthesis of carbon materials and alloy nanoparticles.

(i) A chemical vapor deposition system that uses Joule heating to heat a nickel film on a SiO_2/Si substrate to 900 to 1000°C (using current and voltage range was 15–30 A and 8–12 V) followed by annealing in an argon and hydrogen mixture at a flow rate of 50 sccm. The substrate is then exposed to methane at 50 sccm for 20 to 60 s. 20 s of exposure results in the formation of graphene with a resistance of 600 Ω/square with a 93% transmittance [2].

(ii) A carbothermal shock process uses carbonized silk fabric (CSF) loaded with a solution of transition

metal salts and ethanol (carbon precursor) as a substrate which is treated using joule heating with a pulse voltage of 40 V for 50 ms. The ethanol pyrolyzes to enable the growth of carbon nanotubes on the CSF as it heats up to a temperature of 1700 K in the presence of the metal nanoparticle catalysts [3] (carbothermal shock enabled the facile and fast growth of carbon nanotubes in a second).

(iii) A two-step carbothermal shock that involves rapid heating to a temperature of 2000 K for a shock duration of 55 ms followed by cooling is used to create high-entropy-alloy nanoparticles from metal precursors (several different metal salts) on carbon nanofibers [4] (carbothermal shock synthesis of high-entropy-alloy nanoparticles).

Graphene was first isolated using Scotch tape from bulk graphite in 2004 [5]. The technique used involved peeling graphite layers repeatedly with adhesive tape until a monolayer of pristine graphene stays. The simplicity of the Scotch tape method and its capability of producing pristine graphene flakes has enabled immense research on the properties (refer to Table 1) and consequent applications of graphene. However, the technique is limited for laboratory-scale production due to the tedious process of finding the number of graphene layers under a microscope after peeling and minimal yield [6].

Reduction of graphene oxide (GO) has the potential to rapidly produced inexpensive graphene-based materials at an industrial scale. Utilizing oxidation and reduction reactions, graphite (and other carbon precursors) is converted sequentially into the following derivatives [7]:

(i) Graphene oxide (GO): It was synthesized through oxidizing graphite using an oxidizing agent and an acid, the oxidation leads to segregation of the graphite into monoatomic thick layers while also causing hindrance on the sp^2 bonds [9]. With the sp^3 hybridized carbon bonds out of the original plane and covalent bonding of oxygen-containing functional groups as shown in Figure 1, GO layers are thicker than graphene [8]. The primary prospect of graphene oxide is in nanocomposite fabrication where use of graphene is not applicable. Pristine graphene tends to restack because of its π-π interactions and hydrophobic nature which leads to phase separation within fabricated nanocomposites. The oxygen-containing functional groups in graphene oxide permit better distribution and consolidation. However, the oxygen-containing functional groups require removal to improve electrical conductivity [10].

(ii) Reduced graphene oxide: It has structural similarity to graphene; however, it contains defects, additional carbon ring domains, and a few oxygen-containing groups as shown in Figure 1 [8].

With most research on graphene synthesis processes being applied at the lab scale, there are notable challenges with upscaling to industrial mass production of graphene regarding cost, safety, repeatability, workability, and quality (refer to Table 2). Also, commercialization depends on the viability of graphene to supersede other materials in current products at a competitive cost [1, 15].

Commercial success was first noted with anticorrosion coatings and graphene-reinforced tennis rackets [16]. To expand on this success, it is imperative that [1]

(i) Precise control is ensured over processing techniques, equipment, and parameters for transitioning lab-scale processes to industrial scale.

(ii) Graphene synthesis techniques and products are standardized with respect to quality, purity, and performance parameters.

Even with advances in graphene manufacturing, an economically possible and environmentally friendly synthesis method for mass production of uniform high-quality graphene has not been established, limiting potential industrial applications of graphene. Therefore, this review paper discusses graphene synthesis methods, environmental issues related to graphene production, and the importance of the flash joule heating method of graphene synthesis. When discussing synthesis methods, this paper reviews newly developed graphene manufacturing processes such as layer-engineered exfoliation (LEE), laser-induced graphene (LIG), and flash joule heating. Then, the paper highlights key environmental concerns about mass graphene production followed by the importance of the flash joule heating method for large-scale graphene manufacturing.

2. Graphene Synthesis

Graphene synthesis methods are characterized into the following two categories that are distinguished from the starting material used:

(1) Top-down methods: graphite is the parent material. The primary concept of these methods (summarized in Table 3) is overcoming the van der Waals forces between the graphene layers to produce few-layer or monolayer flakes.

(2) Bottom-up methods: a range of carbonaceous precursors have been used over various bottom-down methods (summarized in Table 3) as the parent material. These synthesis methods use high energy to decompose the carbonaceous material and graphitize the carbon produced to form graphene.

2.1. Top-Down Methods

2.1.1. Mechanical Cleavage. Adhesive tape is used to peel off graphene sheets from graphite. This method enables the production of high-quality sheets but at a low quantity and rate. The number of graphene layers reduces as the sample is repeatedly peeled using the tape [17].

Methods of graphite mechanical cleavage have been explored further from the Scotch tape method to obtain pristine graphene sheets in an industrial-scale capacity.

Table 1: Properties of graphene.

Property	Quantity	Material comparison	Reference
Electron mobility	$2 \times 10^5\ cm^2\ V^{-1}\ s^{-1}$	140 times greater than that of silicon	[11]
Young's modulus	1 TPa	—	[12]
Ultimate tensile strength	130 GPa	100 times greater than that of steel	[12]
Thermal conductivity	4840–5300 W/mK	10 times greater than that of copper	[13]
Optical absorption	2.3%	Ideal substitute for ITO and FTO films	[14]

(i) Oscillating diamond wedge: a sharp diamond wedge is used to cleave off layers of graphene from graphite set in epoxy (refer to Figure 2) [18].

(ii) Layer-engineered exfoliation: metal stressor film is deposited on bulk graphite. The stressor film is then layered with thermal release tape and PMMA to aid the handling of cleavage of the top layer of graphene (refer to Figure 3) [19].

2.1.2. Liquid-Phase Exfoliation. Graphite is added to an aqueous solution or an organic solvent (N-methyl-2-pyrrolidone (NMP)) before it is subjected to an external force (shear mixing, sonication, or ball milling) to overcome the van der Waals forces between the graphene layers resulting in the production of graphene flakes. With ball milling, solid graphite is ground at high speed in a sealed rotating jar having steel balls. The resultant graphene flakes are then dispersed into a liquid. However, shear mixing and sonication are carried out on graphite in a solution. The process can be improved by intercalating the layers using chemicals such as ferric chloride, sulfuric acid, cesium, or potassium [17].

The limitations to this process are that the flakes vary in thickness, i.e., there are variances in the number of layers which results in a low total yield per solvent volume, and extended periods of exfoliation, specifically through sonication, lead to fragmenting and oxidation of graphene [20].

Liquid exfoliation shearing methods are as follows:

(1) Sonication: sound energy is used to produce cavitation [21]. Either using a sonication probe or bath, the liquid solution is agitated to form cavitation bubbles which generate shockwaves upon collapsing [22] (refer to Figure 4). These shockwaves transmit through the graphite which produces tensile stress. Due to multiple cavities, the resultant tensile stress peels off layers of graphene from the graphite [23]. The efficiency of the process and graphene quantity is highly dependent on the geometry of the vessel exposed to the sound energy and the dispersion volume [24]. The graphene produced through sonication has defects due to high pressures and local temperatures generated by the cavitation [25].

(2) High-shear mixing: a rotor-stator or rotating blade is used to move the solution with the graphite at high speed within a region to create shear stress to peel layers of graphene off. For rotor-stator mixing (refer to Figure 5), the production rate (PR) is influenced by the volume, V, of the solution as well as the solution compound [27];

(i) N-methyl-2-pyrrolidone (NMP): production rate is proportional to the volume of NMP solution raised by a factor of 1.1; PR α $V^{1.1}$.

(ii) Surfactant (such as NaC): production rate is proportional to the volume of surfactant solution raised by a factor of 1.6; PR α $V^{1.6}$.

2.1.3. Solid Exfoliation

(1) Ball milling: graphite is placed in a rotating vessel along with the balls. The balls collide with the graphene when the vessel is rotating which results in the layers of graphene exfoliating or fragmenting off the graphite (refer to Figure 6) [26].

(2) Three-roll milling: a mixture of an adhesive (dioctyl phthalate and polyvinyl chloride) and graphite is fed through rollers. The rollers force the graphite to exfoliate into graphene and disperse in the adhesive. The final mixture is added to alcohol and heated to 500°C to remove the adhesive (refer to Figure 7) [29].

2.1.4. Electrochemical Exfoliation. The graphite rod is submerged in an electrolyte (ammonium sulphate ($(NH_4)_2SO_4$)) along with a counter electrode. When a current is passed through the electrodes, the electrolyte intercalates the layers within the graphite rod, causing effective exfoliation of graphene flakes as illustrated in Figure 8. The flakes are then collected through vacuum filtration and dispersed in solvents such as NMP [30]. TEMPO ((2,2,6,6-tetramethylpiperidin-1-yl) oxidanyl) can be added to the electrolyte to prevent hydroxyl radicals (produced via electrolysis of water) from damaging graphene flakes. The flakes have been noted to have minimal defects and high production quantity [17].

2.1.5. Oxidation Exfoliation-Reduction. Graphite is oxidized through a process known as Hummers' method which involves the use of sulfuric acid, sodium nitrate, and potassium permanganate, which produces graphite oxide. Other methods, illustrated in Figure 9, are not rapid and produce graphene oxide with a lower carbon to oxygen ratio. The graphite oxide is exfoliated to produce graphene oxide (GO) flakes which are then treated to produce reduced graphene oxide (rGO). rGO can be produced in massive quantities; however, the inferior quality and use of multiple oxidizing agents and acids require further improvement in this process [32]. When compared to pristine graphene, graphene oxide

Table 2: Challenges in industrial-scale graphene synthesis [1].

Factor	Challenges
Quality	Commercially available graphene flakes lack uniformity in both size and number of layers with varying degrees of impurity and defects
Cost	High energy consumption, specialized equipment, thermal annealing, and filtration accumulate the price of producing graphene on a large scale
Repeatability	Quality and properties of graphene varies depending on the source material (existing structural defects) and synthesis conditions (process parameters and equipment)
Workability	Commercially available graphene products are only 50% actual graphene which hinders potential applications. Poor repeatability has also restricted applications to use in composites where consistency is not a priority
Safety	Use of chemicals (oxidizing agents and surfactants) in certain graphene synthesis processes are hazardous and/or cause pollution

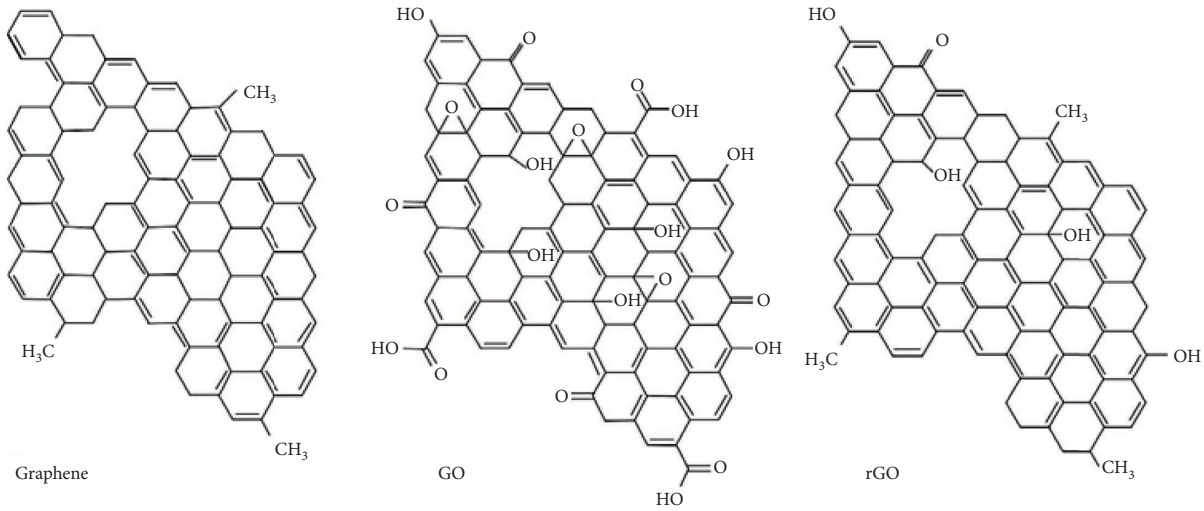

Figure 1: Structure of graphene, graphene oxide (GO), and reduced graphene oxide (rGO) [8].

is a poor electrical conductor because of the presence of oxides and reduced graphene oxide contains structural defects after the reduction process that in turn degrades structural and electrical properties [20]. The oxidation exfoliation method is applicable to a range of carbon precursors.

(i) Carbon nanofibers: the nanofibers are subjected to Hummer's method [33].

(ii) Charcoal: carbonaceous waste material such as leaves, wood, bagasse, bones, and animal waste are subjected to approximately 500°C while wrapped in aluminium foil for 5 days. The resulting charcoal ground up, rewrapped in foil, and heated for 24 hours at 450°C. Then, a gram of the carbonized material is added to 100 ml of distilled water with 0.5 grams of iron (III) chloride hexahydrate with the addition of hydrochloric acid to maintain a pH of 2. The solution is mixed for 5 hours at 60°C followed by evaporation of water at room temperature over 5 days. Lastly, the remnants are dried for 5 hours at 100°C resulting in graphitized solid material. The material is then subjected to a modified Hummer's method to produce graphene [34].

(1) Methods of graphene oxide reduction [10]

(1) Hydrazine hydrate:

Graphene oxide is reduced using hydrazine monohydrate ($N_2H_4{\cdot}H_2O$) to produce reduced graphene oxide with structural and electrical properties near equivalent to pristine graphene. With the temperature of the reduction reaction being influential, a study showed that reducing graphene oxide at 95°Celsius for 3 hours resulted in reduced graphene oxide with a carbon to oxygen ratio of 15 : 1 and an electrical conductivity of 5 S cm^{-1} [36].

(2) Catalysts:

Zinc and aluminium functions as a reduction catalyst in hydrochloric acid. The metal catalyst reacts with the acid to form hydrogen gas and metal chloride. The hydrogen gas exothermically reacts

Table 3: Summary of graphene synthesis methods.

Type	Method	Process	Final product and applications	Advantage	Disadvantage	Reference
Top-down methods	Mechanical cleavage	A film of gold is deposited on graphite surface through thermal evaporation. PMMA poly (methyl methacrylate) and thermal release tape is used to lever the gold film. Due to the binding energy of the gold and graphite being greater than the interlayer binding energy in graphite, the tensile stress induced from peeling off the film causes spalling of the top layers of graphene. Graphite is first set in epoxy and then a diamond wedge mounted on an ultrasonic oscillation system is used to cleavage off required thickness of graphene	Pristine monolayer graphene: used in graphene analysis for labs, primarily due to high quality	Pristine single layer graphene sheets. Control on graphene thickness	Size of graphene is limited by surface size of graphite. Ideal metal depositions (as known as stressor film) are rare and/or precious metals (gold, cobalt)	[17–19]
	Liquid phase exfoliation	Graphene is sheared of using external forces (using shearing rotors, ball milling, or sonication) in a surfactant solution (primarily N-methyl-2-pyrrolidone (NMP))	Pristine few-layers graphene nanoplatelets: used as composite filler inks and conductive coats	High-quality few-layer graphene dispersion. Scalable process. Better thermal and electrical conduction than reduced graphene oxide	Edge defects. Separation of graphene from solution required for certain applications usually through centrifuge	[20, 23, 24, 27, 28, 32, 33, 78, 79]
	Solid exfoliation	Graphene layers are sheared off from graphite either through use of ball milling or rollers with oxalic acid (reducing agent). The resultant graphene sheets are subjected to thermal annealing in buffer gases (argon, nitrogen, and hydrogen) to restore graphitic lattice structure and reduce oxygen groups	Few-layer graphene nanosheets: used in paints, composites, and inks	Allows mixing of graphene with other materials for composites. Graphene functionalization	Nonuniform flake size and thickness with edge defects and impurities (from metal chipped off balls and high extensive impacts)	
	Intercalation exfoliation	Graphite is added to an intercalation solution and/or electrolytic solution (eutectic salt, Li/PC, $(NH_4)_2SO_4$, H_2SO_4, H_2O_2, ionic liquids) in conjunction with electrochemistry or heat. As the intercalation solution reacts, gases produced causes the graphite to expand. The expanded graphite is sonicated in water, NMP, or DMF to produce graphene nanosheets in a solution	Few-layer graphene nanosheets: used in anticorrosive coats, battery components, composites, and rubbers	Scalable process. Enables functionalization of graphene. Graphene flakes have been noted to have minimal defects	Expensive ionic liquids. Time-intensive process	
	Oxidation exfoliation reduction	Graphite is oxidized (using oxidizing agents such as $KMnO_4$, $NaNO_3$, H_2SO, and HNO_3) to introduce oxygen groups which increases the space between the layers of graphene. With the interlayer van der Waals forces reduced; the graphite oxide is exfoliated into few layers of graphene oxide (GO). Exfoliation is achieved through sonication or stirring in a surfactant solution (NMP, H_2O, N, and N-dimethylformamide (DMF)). Graphene oxide nanosheets undergo reduction to produce reduced graphene oxide (rGO) through: thermal annealing in buffer gas or vacuum. Hydrothermal reduction: low concentration of GO aqueous solution is subjected to high pressure and temperature. Chemical reduction using either hydrazine, sodium hydroxide, potassium hydroxide, or sodium borohydride	Few-layer reduced graphene oxide (rGO): used in anticorrosive coats, battery components, composites, and rubbers	Scalable process. Enables functionalization of graphene	Use of hazardous chemical. Time-intensive process. Produced graphene requires washing and treatment to remove chemicals. Process has poor repeatability. Prominent defects in rGO due to oxidation	
	Arc discharge	Graphite rods set a few millimeters apart are exposed to buffer gases (hydrogen, helium, nitrogen, argon, or a mixture of those gases) in a stainless-steel vessel. Direct current is passed through the rods which produces an arc plasma. The rods vaporize from the high temperatures from the plasma and cool form graphene nanoflakes	Graphene nanoplatelets used in lubricants, composites, inks, and coats	Catalyst not required. Highly suited for producing graphene at a rate of decagrams per hour	Low yield. Amorphous carbon impurities. Required annealing which increases processing time	[53–55, 80]

Table 3: Continued.

Type	Method	Process	Final product and applications	Advantage	Disadvantage	Reference
Bottom-up methods	Chemical vapor deposition	Carbonaceous substance (commonly methane gas) is pyrolyzed at high temperatures (with a mixture of argon and hydrogen gases) to produce carbon which deposits on a metallic substrate (copper or nickel) to form graphene films	Monolayer or few-layer graphene films used in optoelectronics, sensors, and touch panels	High-quality large graphene films. Potential for upscaling process	Process is expensive (high energy required). Removal of catalyst and transferring of graphene onto suited substrate	[58, 59, 61]
	Epitaxial graphene	Layers of graphene can be grown on silicon carbide (SiC) crystal by thermal decomposition at temperatures greater than 1000°C under an ultrahigh vacuum	Few-layer graphene wafer: used as conductive films and transistors	High-quality large-area graphene wafer. SiC crystal on which graphene is grown on is a highly suited substrate for applications in electronics	Energy intensive process. SiC is expensive	[56, 57, 81]
	Unzipping carbon nanotube	Carbon nanotubes are split open using acids and oxidizing agents (sulfuric acid and potassium permanganate), intercalation compounds (ammonium and lithium), metal nanoparticle catalyst, electric current, and argon plasma	Graphene nanoribbons: used in composites, electronics, and spintronics	Size of graphene nanoribbons can be controlled by selection of nanotube	Oxidation and defects evident along edge where splitting occurs. High cost of chemicals and precursors	[62–67]
	Laser-induced graphene	CO_2 laser is used to irradiate polyimide substrate in ambient conditions and natural resources in either an inert atmosphere or ambient conditions to produce porous graphene	Porous graphene: used in electronic devices such as sensors and capacitators	Process allows for control of morphology and patterning of graphene	Laser irradiation of certain materials at ambient conditions results in ablation and thermal damage	[68]
	Rapid thermal annealing	A carbon source and metal catalyst are deposited (either chemically or electrochemically) on a pretreated substrate (Si, SiC, SiO_2, or Cu) which undergoes rapid thermal annealing at high temperatures either under vacuum or in an inert atmosphere	Monolayer graphene films: flexible displays, thin film for photovoltaics, and printable electronics	Shorter processing time. Allows for modification and improvement of graphene-based materials and films	Impurities on substrate can affect the quality of graphene. Use of metal catalyst or substrate requires a strong acid to separate it from the graphene. This can result in defects and impurities	[69, 82]
	Gas-phase-synthesized graphene	A carbonaceous fluid such as ethanol is subjected to an argon plasma generated by microwaves at atmospheric pressure	Graphene nanoplatelets: used in lubricants, composites, inks, and coats	Substrate not required. Process performed at atmospheric conditions	In-depth statistical analysis of dependency of production variables (plasma gas flow rate, microwave forward power, carbon precursor material composition, and flow rate) has not been investigated through design of experiments	[72–75]

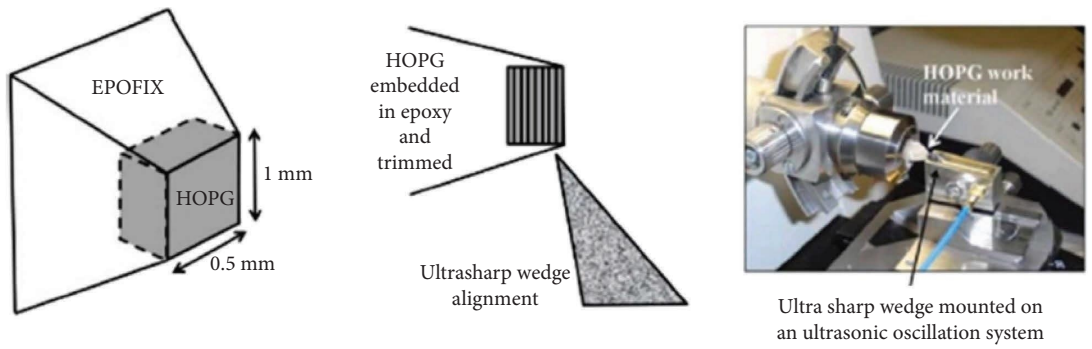

Figure 2: Diamond wedge method [18].

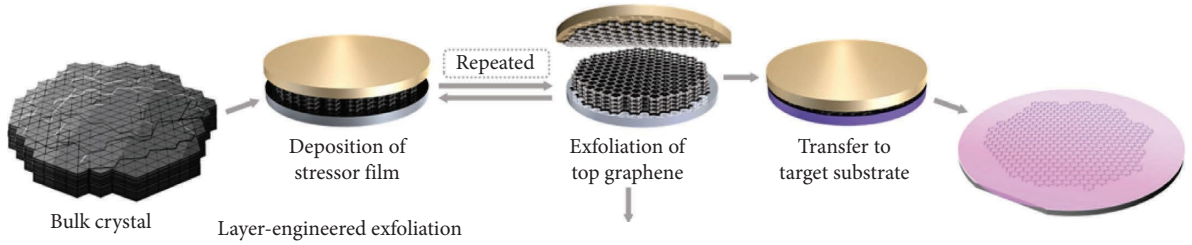

Figure 3: Layer-engineered exfoliation process [19].

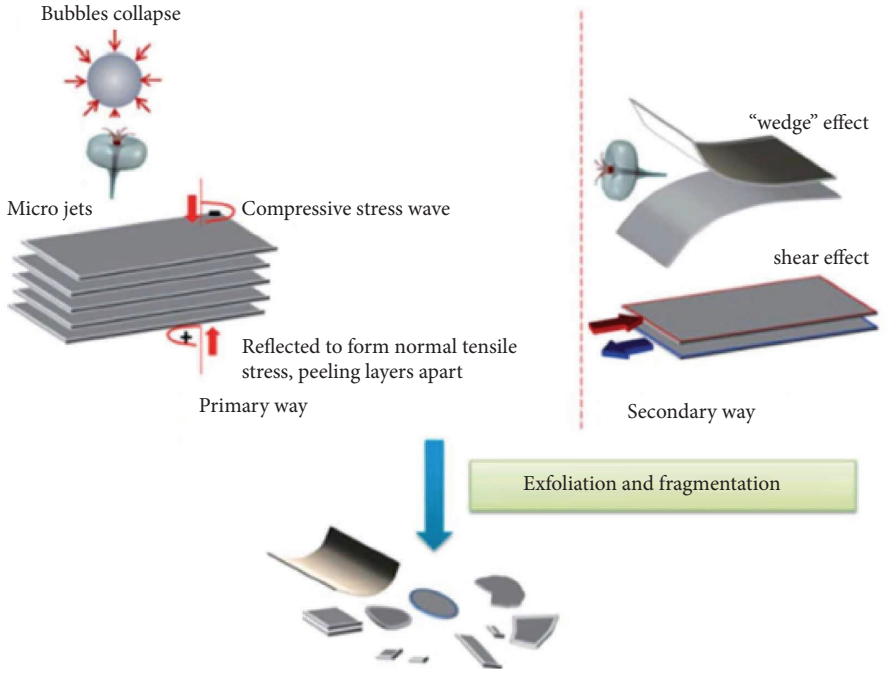

Figure 4: Working principle of sonication [26].

with the oxygen in the graphene oxide to produce reduced graphene oxide. The resulting reduced graphene oxide shows an electrical conductivity of 2.1×10^3 Sm^{-1} [37–39].

(3) Organic solvents:

Graphene oxide dispersions made with organic solvents such as DMF are reduced at 463 K for an hour. The DMF breaks down to carbon monoxide and dimethyl amine. The resulting carbon monoxide is a strong reducing agent which reacts with the oxygen from the graphene oxide to form a dispersion of reduced graphene oxide [40].

Graphene oxide prepared from graphite using the Hummer's method can be heated in situ with oxidizing agents at 393 K for 2 hours to produce reduced graphene oxide dispersion. The resulting

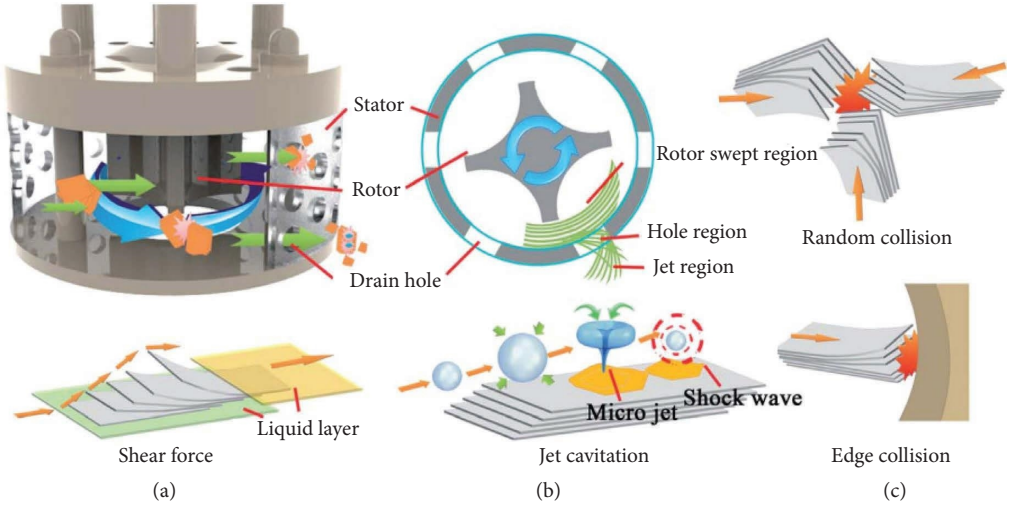

Figure 5: Rotor-stator mixing [28].

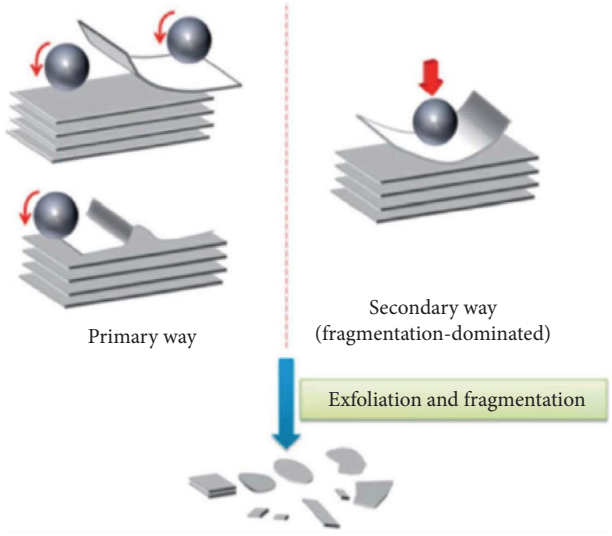

Figure 6: Ball milling mechanism [26].

reduced graphene oxide was highly electrochemical stable and 1000 times more conductive than graphene oxide [41].

(4) Sodium compounds:

A multitude of sodium based reductants have been utilized to produce reduced graphene oxide. Sodium borohydride has been used to reduced graphene oxide dispersions in ambient conditions in the presence of silver nano particles. The sodium borohydride hydrolyses to form borohydride which oxidizes on the surface of the silver nano particles which leads to the transfer of electrons on said silver nanoparticles. The electrons are then transferred to graphene oxide and initiates reduction resulting in reduced graphene oxide. When sodium borohydride reacts in an alkaline condition, that is, in the presence of sodium hydroxide, a stable dispersion of reduced graphene oxide which can be formed into films through vacuum filtration with an electrical conductivity range from 10 to 1500 S cm^{-1} [42].

(5) Laser:

A laser with a spot diameter of 1064 nanometres and power of 50 microwatts most efficiently reduced graphene oxide at a scan speed of 30 mm/s under nitrogen along with potassium hydroxide. Theoretically, the laser is capable of inducing ocalized annealing temperatures of up to 1273 K for a few nanoseconds which is the causation oxygen-containing functional group decomposition on

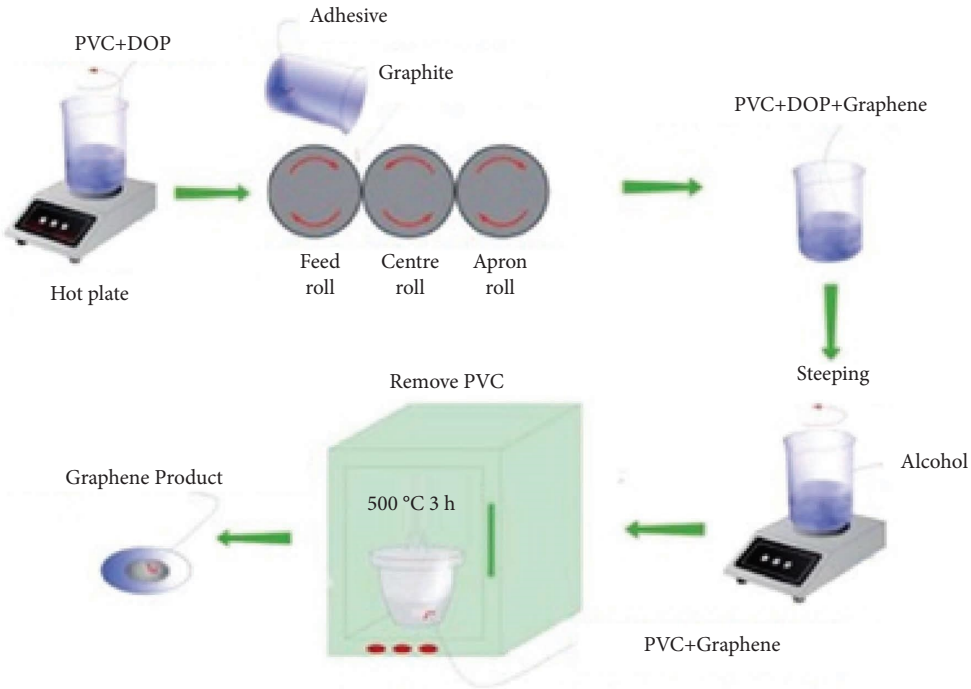

Figure 7: Three-roll milling [29].

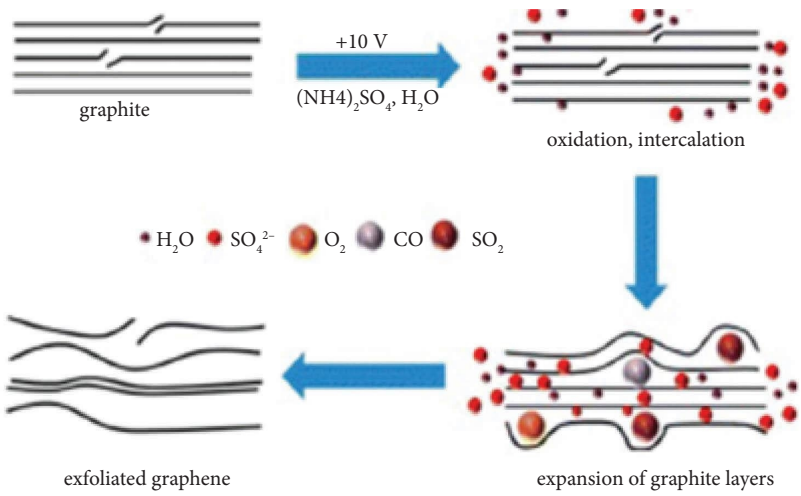

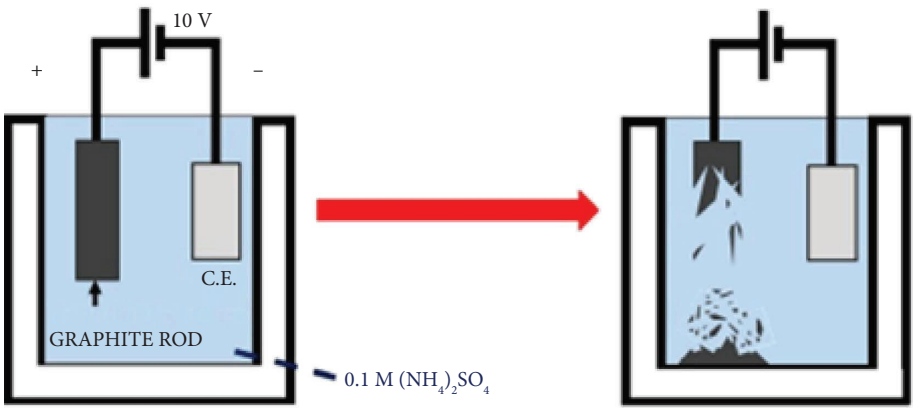

Figure 8: Electrochemical exfoliation mechanism and equipment setup for electrochemical exfoliation [31].

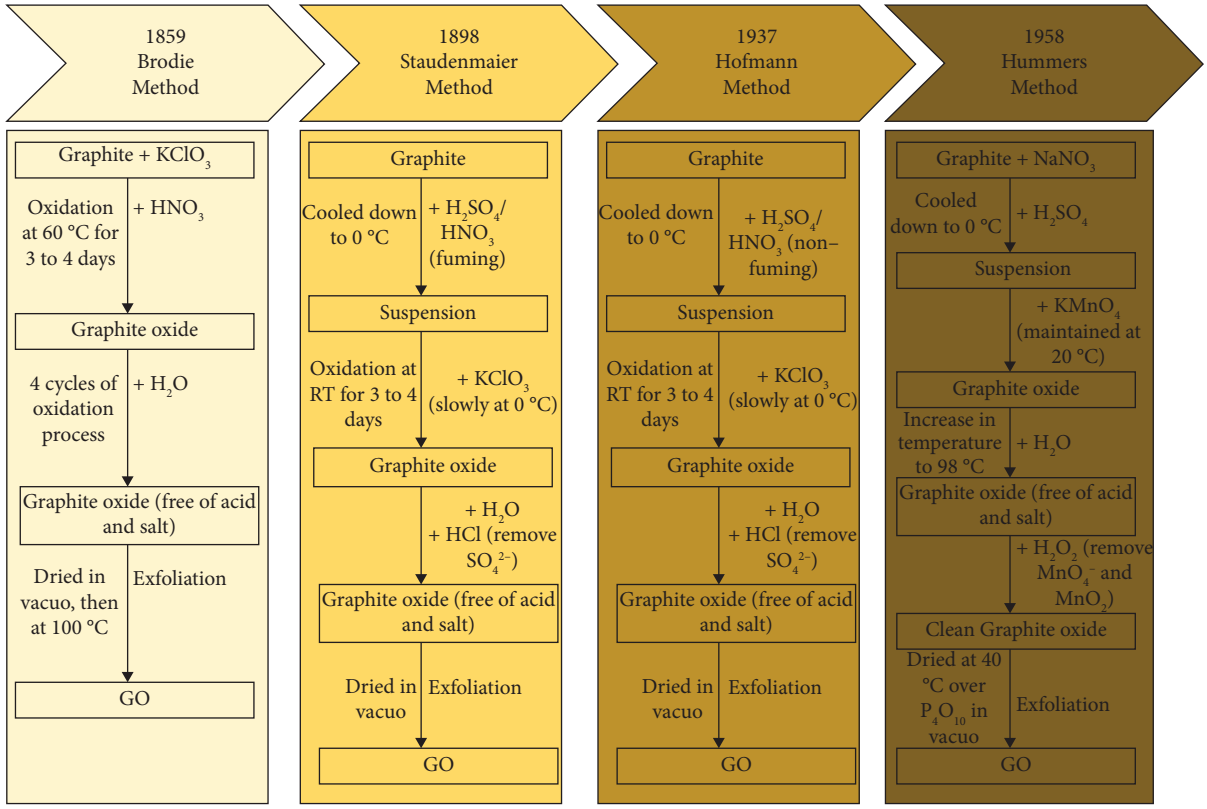

Figure 9: Methods of oxidizing graphene [35].

graphene oxide, hence producing reduced graphene oxide [43].

(6) Plasma:

A scanning atmospheric plasma at 300 Watts for an exposure time of 90 seconds has multiple reduction methods through the generation of charged ions. The resulting charged ions inelastically collide with the graphene oxide which ruptures the oxygen-containing groups to produce oxygen ions that react with surrounding oxygen species to form oxygen. Another mechanism involves interaction of free electrons from the plasma with oxygen in the surrounding atmosphere to produce oxygen absorbates. The absorbates transfers its free electrons to the graphene oxide surface thus producing reduced graphene oxide with improved doping. Finally, nitric oxide forms in the hot plasma zone from atmospheric nitrogen and oxygen. The highly reactive nitric oxide with the oxygen-containing groups on graphene oxide surface to form reduced graphene oxide and nitrogen dioxide [44].

(7) Photocatalysis:

Photocatalytic graphene oxide reduction has two major approaches:

(i) The use a photoinitiator that is activated using ultraviolet: When exposed to ultraviolet irradiation at 100 mW cm^{-2} (with a spot diameter of 395 nm), the photo-initiator, such as phenylbis (2,4,6-trimethylbenzoyl) phosphine oxide, produces free radicals which reacts with the oxygen functional groups to produce reduced graphene oxide with an electrical conductivity of ~3.7 × 103 S m^{-1}. The reaction is conducted with an oxygen inhibitor (monoethanolamine) to improve photoreduction reaction through quenching of molecular oxygen [45].

(ii) The use of photoactivatable inorganic nanoparticles such as silver nanoparticles: The silver nanoparticles are the photocatalyst that reduces graphene oxide in the presence of surface plasmon resonance induced visible light and dimethylformamide (DMF) as an electron donor. A 400 Watt Xe lamp at wavelength greater than 420 nm is exposed to a mixture of silver nanoparticles, graphene oxide, and DMF for 40 minutes to produce silver-reduced graphene oxide aggregates with a sheet resistance of 9000 Ω/sq. [46].

(8) Thermal:

Utilizing thermal annealing to reduce graphene oxide produces reduced graphene oxide with varying electrical and structural properties. Determination of reduction temperature is the end application of the reduced graphene as annealing temperature affects reduction extent and structural decomposition of the graphene plane. At 573 K, graphene oxide releases water, carbon dioxide, and carbon monoxide due to graphene oxide basal plane decomposition leading to carbon bond cleavage [47].

Annealing at a temperature of 3000 K results in activation of bridged ether bonds and carbon to carbon bonds situated near hydroxyl groups which produces large carbon rings. With a continuous increase in temperature, the carbon backbone breaks which leads to an amorphous state. This is prominent at temperatures of 5000 K where there is an increase in sp^2- hybridized carbon atoms [48].

(9) Microwave:

Microwave inducted reduction of graphene oxide starts off with removal of carbonyl groups at less than 600 K followed by the hydroxyl group at 1500 K and then the carboxyl groups at near 2200 K. Finally, the epoxy groups are removed at 2800 K. The process is limited in its reducing ability as the oxygen-containing functional groups located on the edges of the sheet could not be removed due to structural decomposition of reduced graphene oxide that would result from required temperatures. The final product contains minimal to no oxygen-containing functional groups and is achieved in a brief time with the convenience of having control over reduction temperature [49].

(10) Hydrothermal:

Hydrothermal reduction occurs through hydroxyl group dehydration using an acid catalyst (with water being the source of positively charge hydrogen ions). In acidic conditions, the carboxyl groups and hydroxyl groups undergo protonation resulting in reduced graphene oxide sheets to aggregate through H-bonding or π-π interactions. The process is conducted at 453 K for 6 hours [50].

(11) Electrochemical reduction (ECR):

There are primarily two methods of electrochemical reduction of graphene oxide:

(i) The one-step process involves in situ electrochemical reduction of colloidally dispersed graphene oxide in an electrolyte. This forms thin films of reduced graphene oxide on an electrode. The electrolyte conductivity (ideally between 4–25 $S\,m^{-1}$), pH (less than 10), and applied potential (~0 to −1.5 V) govern the efficiency of reduction process.

(ii) The two-step process which requires a coating of graphene oxide on the electrode surface first, and then, it is reduced using electrochemical process that utilizes a three electrode system in an electrolyte.

The properties of the resulting reduced graphene oxide from the first method are dependent on the applied potential while in the second method, reduced graphene oxide films of uniform shape, size, and thickness can be produced by controlling initial depositing conditions of graphene oxide [51, 52].

2.1.6. Arc Discharge Method. The arc discharge method consists of graphite rod anode and cathode that are exposed to buffer gases in a vacuum vessel, inert gases, or air. A constant current is passed through the electrodes from a DC power supply resulting in plasma formation (which reaches a temperature from 3727–5727°C [53]) between the cathode and anode (refer to Figure 10). The graphite anode vaporizes into the plasma forming graphene [54].

2.2. Bottom-Up Synthesis

2.2.1. Silicon Carbide Sublimation (Epitaxial Growth). Layers of graphene can be grown on silicon carbide (SiC) crystal by thermal decomposition at temperatures greater than 1000°C under an ultrahigh vacuum. As the SiC crystal is heated, it decomposes to its constituents silicon and carbon. The silicon vaporizes off from the crystal surface while the carbon atoms form graphene layers. The graphene grown on the Si-terminated surface of SiC are of high quality, ordered crystalline films, with minimal wrinkles [1]. The major drawbacks of this method are the elevated temperatures required to decompose SiC and the limited size of graphene films due to the excessive cost of SiC wafers. This has limited the use of epitaxially grown graphene for selected electronics such as high-frequency transistors [56].

Hexogonal SiC crystals used for graphene synthesis have are made of Si-terminated (0001) surface and C-terminated $(000\overline{1})$ surface as shown in Figure 11. The process begins with the sublimation of silicon atoms along the step edge. This is because the silicon atoms at the step edge have more dangling bonds compared to the silicon atoms found at other surface zones or within the crystal. The carbon atoms that stay on the edge form a graphene nucleus continues to grow laterally towards the upper surface of the step edge (Figures 12(b)–12(d)). The same graphene growth from the lower surface joins with the graphene produced at the step (Figures 12(e) and 12(f)). The first carbon layer is a buffer layer which is then followed by a layer of graphene (Figures 12(h) and 12(g)) [57].

The difference between the graphene growth on the silicon-face (0001) and the carbon-face $(000\overline{1})$ is that the graphene layers formed on the $(000\overline{1})$ surface are stacked in a disorderly manner (turbostratic), while on the (0001) surface, the graphene showed ABC stacking. Graphene from carbon-face $(000\overline{1})$ SiC also has high charge-carrier mobility, weaker coupling to the SiC surface and greater defects (Figure 13(f)) than graphene from silicon-face (0001) [57].

2.2.2. Chemical Vapor Deposition. A carbon-rich source (hydrocarbons) is thermally decomposed at elevated temperatures and the carbon atoms graphitize on a substrate which is usually transition metals such as copper or nickel. To

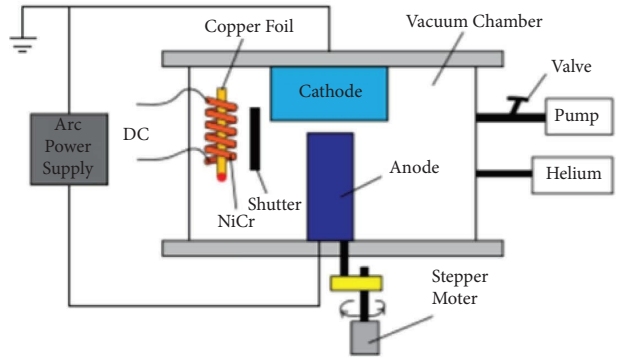

Figure 10: Arc discharge method [55].

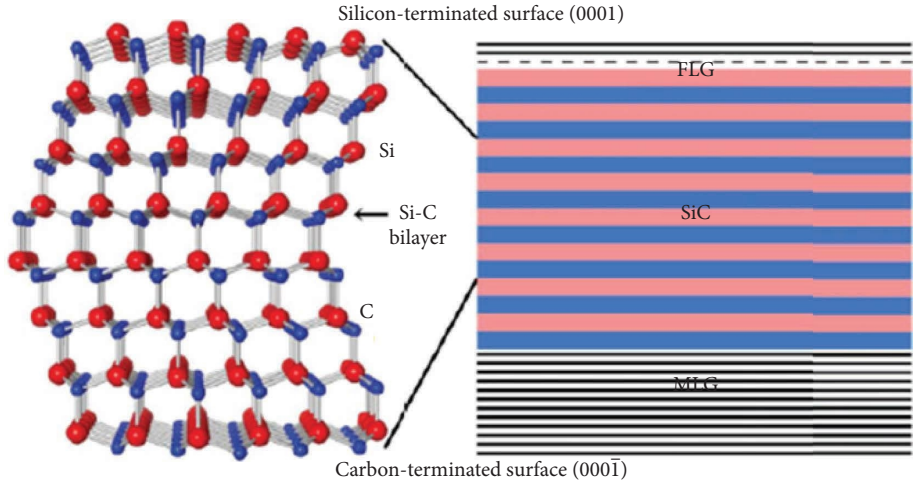

Figure 11: SiC crystal with reference to (0001) surface and (000$\bar{1}$) surface [57].

produce monolayer graphene, copper is used due to low carbon solubility and moderate catalytic activity. The graphene film is then transferred onto a transferring substrate (usually silicone or silicon dioxide) with the use of support polymers (primarily polymethylmethacrylate (PMMA)). Using ferric chloride ($FeCl_3$), the copper substrate is etched to allow the PMMA and the graphene to be placed on a target substrate. Finally, the PMMA supports are removed using acetone [17].

The process involves the formation of few-layer graphene from a carbon-rich source material over a catalytic metal substrate at elevated temperatures. The carbon-based source decomposes to release the carbon which is then either absorbed by the metal substrate (such as nickel and cobalt) and then precipitated as graphene or undergoes nucleation and grows graphene on the surface of the metal substrate (such as copper). The governing parameters that affect the graphene produced are as follows [59]:

(i) Concentration and exposure of carbon over the substrate

(ii) Flow rate of the carbon-rich source material

(iii) Cooling rate

(iv) Type of carbon-rich source material

Taking copper as the substrate and methane (CH_4) as the carbon-rich source material, CVD synthesis process involves [60]:

(i) Methane decomposes to form C_XH_Y species on the surface of the copper substrate which is in a methane/hydrogen atmosphere (Figures 14(a) and 14(d)).

(ii) As the copper is supersaturated with C_XH_Y, nuclei begin to form (Figures 14(b) and 14(c)).

(iii) These nuclei form zones of graphene on the copper surface (Figure 14(e)).

(iv) As those zones grow and join with each other, the copper surface gets covered by graphene while the undecomposed methane and by-products are removed from the chamber (Figure 14(f)).

An example of the processing parameters and conditions are as follows:

(i) Preannealing for 1 to 2 hours, the copper substrate in a furnace is set at 1000°C that has been backfilled with hydrogen gas (or a mixture of hydrogen and argon) while keeping a hydrogen flow at 50 sccm.

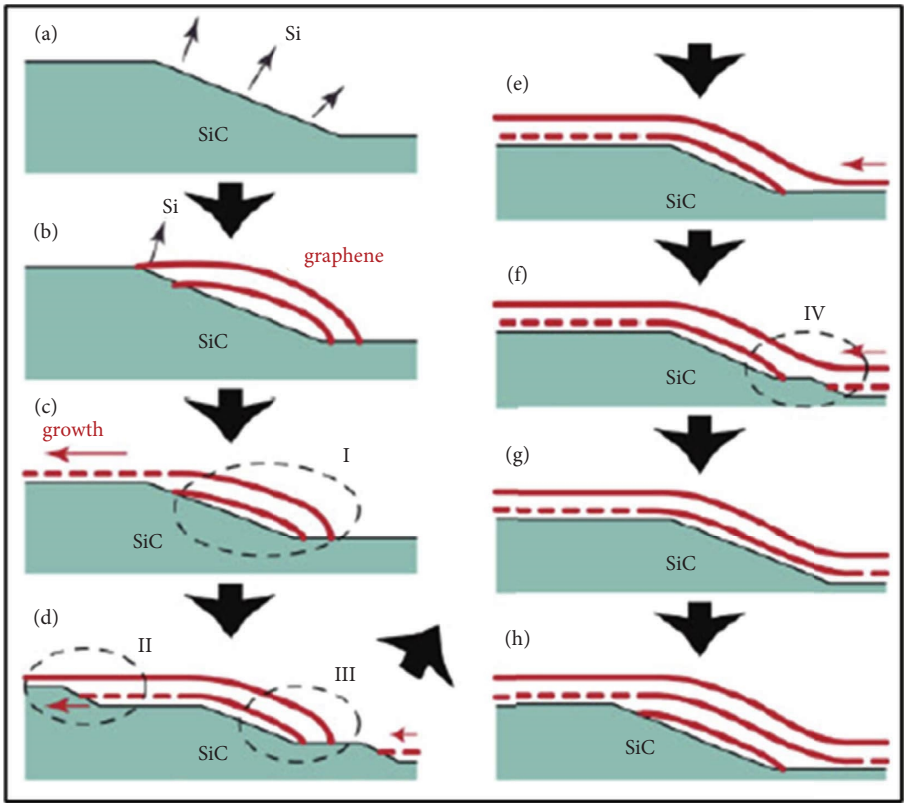

Figure 12: Graphene growth on silicon carbide (0001) surface [57].

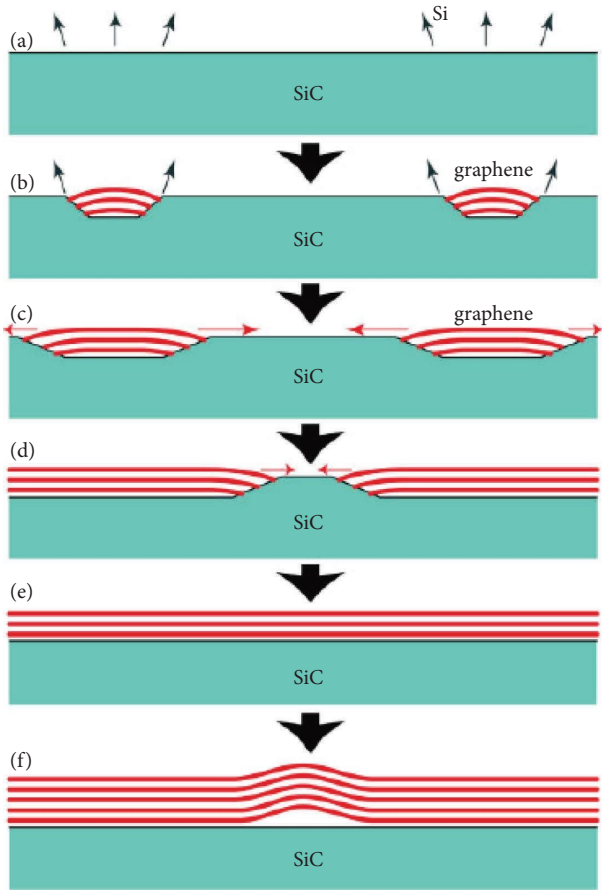

Figure 13: Graphene growth on silicon carbide $(000\bar{1})$ surface [57].

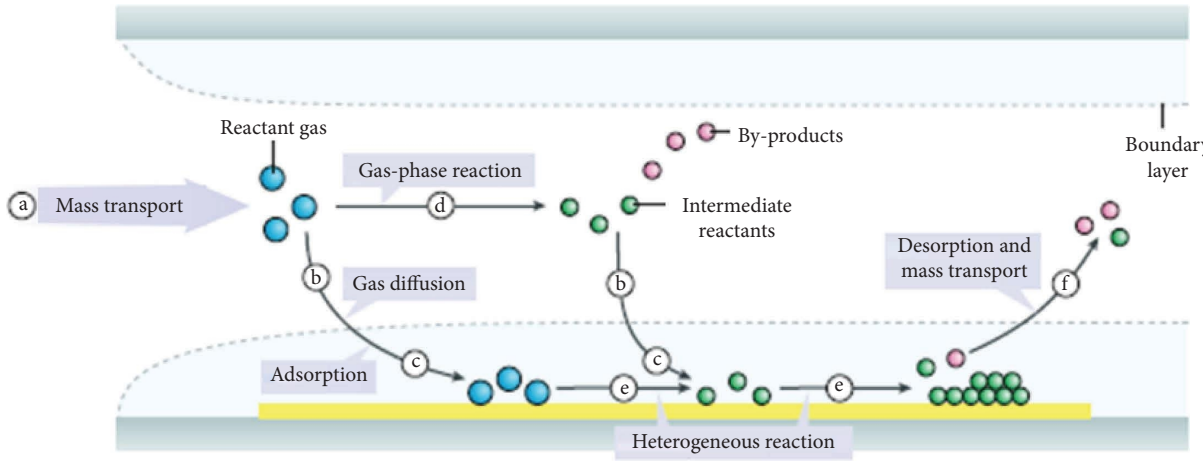

Figure 14: Graphene growth mechanism in CVD [58].

(ii) Methane at a flow of 35 sccm is introduced for a growth time of 5–20 min.

(iii) Then, the furnace is allowed to slowly cool to room temperature with the hydrogen atmosphere [60].

CVD can produce high-quality graphene films. However, the process is expensive and not readily scalable. There is also a need to improve manufacturing and product parameters which are as follows [61]:

(i) Achieving graphene growth at lower temperatures rapidly.

(ii) Attaining a high degree of uniform crystallinity with better oriented crystalline.

(iii) Developing scalable graphene transfer techniques.

In terms of upscaling the graphene film production, two processes have been designed [17]:

(i) Roll to roll (R2R) produces a continuous graphene film (refer to Figure 15).

(ii) Batch to batch (B2B) produces graphene wafers.

2.2.3. Unzipping Carbon Nanotubes. Carbon nanotubes (CNTs) are split open using various methods (Figure 16) to produce graphene nanoribbons:

(a) Intercalation and exfoliation: multiwalled carbon nanotubes (MWCNT) are added with lithium and liquid ammonia. The Li-NH_3 complex with dilute hydrochloric acid and heat intercalates and splits the MWCNT walls [62].

(b) Chemical: MWCNT is suspended on concentrated sulfuric acid and treated with potassium permanganate (500 wt.%) for an hour at room temperature followed by another hour at 55–70°C [63].

(c) Catalytic: CNT catalytically unzipped with lead nanoparticles in an oxygen liquid medium under microwave irradiation [64].

(d) Electrical: an MWCNT is contacted by a moving electrode with a current passing through it which ruptures the outer layer of CNT [65].

(e) Physiochemical: MWCNT split using hydrogen plasma reaction at 300°C [66].

2.2.4. Laser-Induced Graphene (LIG). Laser irradiation transforms carbonaceous materials such as polyimide (PI) into graphene under ambient conditions. A 4.8 W laser produces graphene of the highest crystallinity, fewer defects, and the largest domain size on a PI. The minimum required energy to start graphene formation on PI was noted to be approximately 5.5 J/cm^2. LIG morphology can be controlled through pulses per inch (PPI), lines per inch (LPI), and laser spot size.

(i) 1000 PPI × 1000 LPI with 100 μm laser spot size: LIG has an in-plane porous structure.

(ii) 500 PPI × 500 LPI with 60 μm laser spot size: LIG forms as out-of-plane fibers.

Figure 17 shows the set up used when producing LIG from wood where it is lasered in an inert atmosphere to prevent ablation [68].

2.2.5. Rapid Thermal Annealing. A metal catalyst (nickel, copper, Ni-Cu alloy, or cobalt) is deposited onto a substrate (silicon, silicon carbide, silicon dioxide wafers, or copper films) along with a carbon source which is annealed at elevated temperatures (500–1000°C) under low vacuum as illustrated in Figure 18 [69].

(1) Thermal evaporation: nickel is deposited on a SiO_2 substrate in a vacuum (10–6 mbar) through evaporation.

(2) Pulsed laser deposition: a laser ablates a carbon source to deposit amorphous carbon on the substrate in a vacuum chamber (10–7 mbar).

(3) Rapid thermal heating: the substrate is heated to an elevated temperature (900°C) for 420 seconds at a 10–2 mbar vacuum to induce graphene growth.

(4) Nickel etching: $FeCl_3$ is used to remove nickel to produce transfer-free graphene.

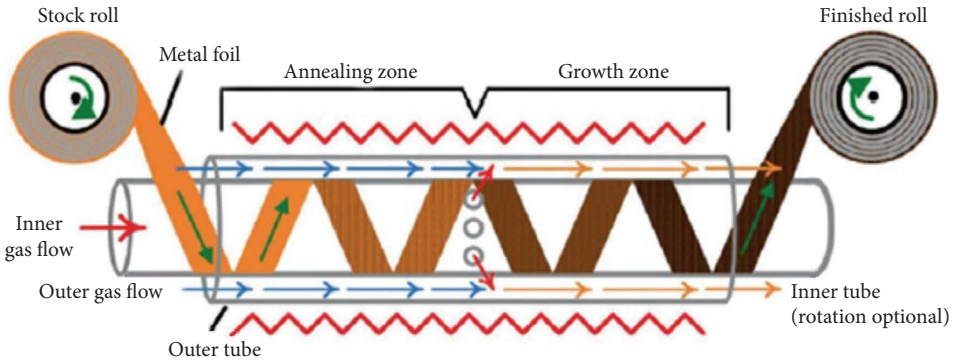

Figure 15: Roll to roll CVD graphene production [16].

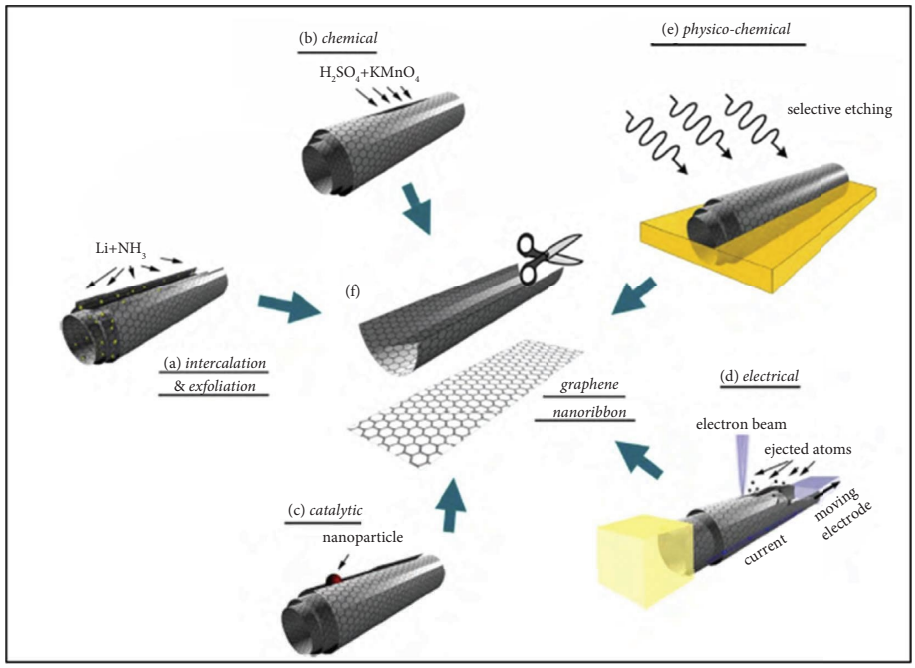

Figure 16: Methods of unzipping carbon nanotubes [67].

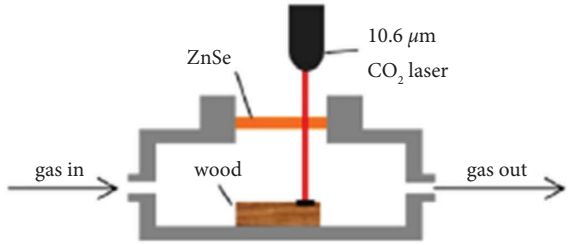

Figure 17: LIG synthesis on wood [68].

2.2.6. Gas-Phase-Synthesized Graphene (GSG). A carbonaceous gas (ethanol) is subjected to a microwave inducted argon plasma at atmospheric pressure [70, 71]. The ethanol and argon mixture enter the section of the quartz tube where the plasma electrons absorb the microwaves which transfer the energy to heavier particles through collisions. This results in an electron dense environment (greater than 10^{13} cm^{-3}) where gas temperatures reach 3000 K [71–74]. The ethanol decomposes into reactive fragments that flow out of the quartz tube to plasma afterglow where it reacts to form GSG (Figure 19) [74].

Top-down and bottom-up graphene synthesis methods discussed in Section 2 are summarized in the following table (Table 3) for a detailed understanding of the readership.

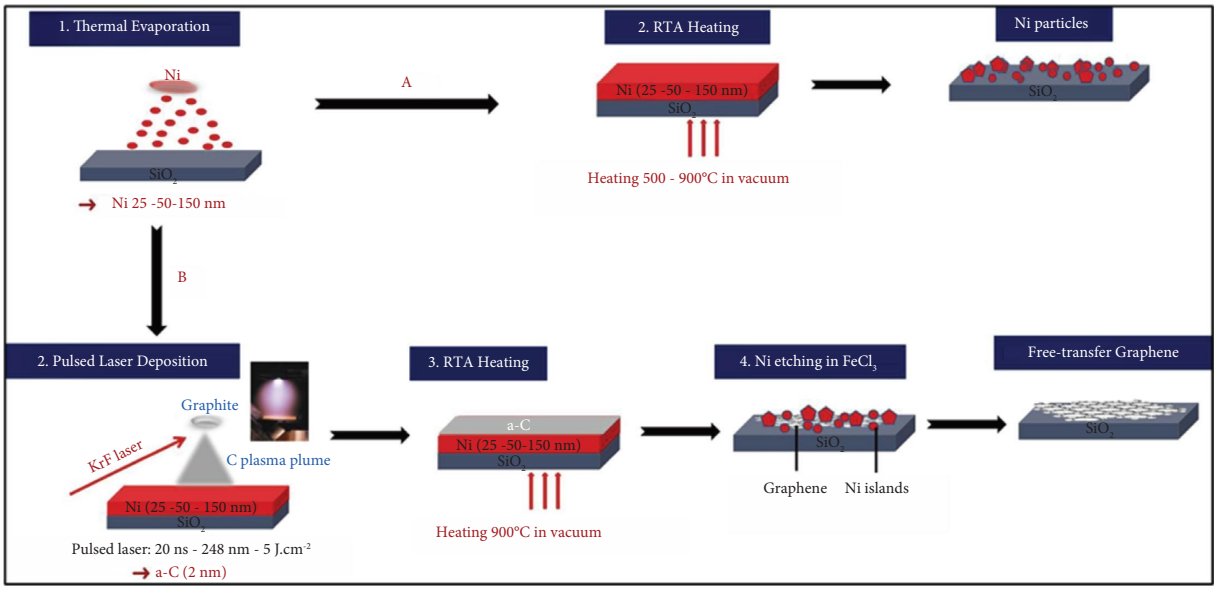

Figure 18: Rapid thermal annealing synthesis route [69].

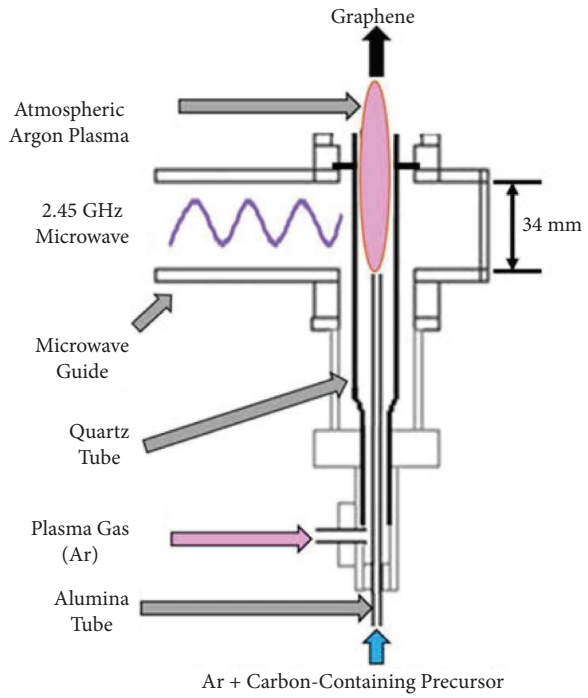

Figure 19: Microwave plasma reactor for GSG production [75].

3. Turbostratic Graphene Produced through Flash Joule Heating (FJH)

This bottom-up approach converts carbonaceous material to turbostratic graphene using high current electric pulse discharges using a capacitor bank. The carbonaceous material is compacted in a quartz tube between two electrodes which are connected to a capacitor bank circuit as shown in Figure 20.

An AC-DC converter supplies a DC voltage to charge the capacitor bank. The lamp connected parallel to the capacitor bank shows when the capacitors are fully charged. An insulated-gate bipolar transistor (stated as a power switch in Figure 19) with a custom LabView program is used to control the time of discharge. The flash chamber is where the carbonaceous material is compressed between electrodes in a desiccator under a slight vacuum to aid in the expulsion of heteroatoms and hydrogen through the clearance between the electrodes and the quartz tube [76].

Amorphous carbon black powder is compressed between electrodes in a quartz tube and subjected to a slight

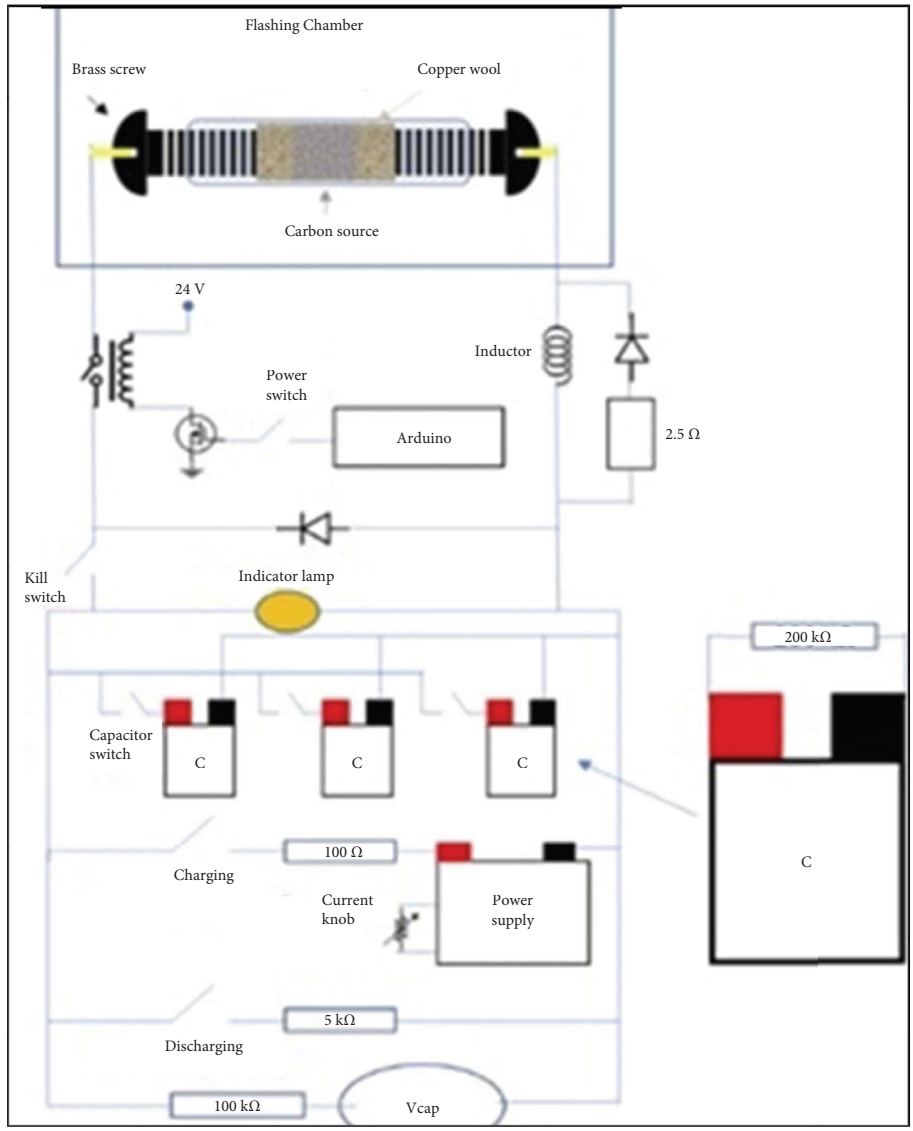

Figure 20: Electrical circuitry for FJH graphene [76].

vacuum of −10 mm Hg to aid in the sublimation of heteroatoms and hydrogen (however, the process is possible at atmosphere pressure). While in flash joule heating, the content in the quartz tube must reach a minimum temperature of 3000 K to ensure effective conversion of the carbon black into high-quality turbostratic graphene. This was achieved through utilizing a 60-mF capacitor bank discharging 110–120 V for a flash duration of 30–100 ms (with a discharge time of 50 ms) when working with 0.03 g of carbon black. The quality of the turbostratic graphene is clear in the Raman spectra in Figure 20 [76, 77]:

(i) At capacitor voltages less than 90 V, the flash graphene produced had significant structural defects shown by the high D peaks in the Raman spectra.

(ii) Optimal capacitor voltage is shown to be 110 V with a higher I_2D/G and low ID/G (indicative of low defect concentration).

(iii) The graph shows the ideal temperature and flash duration, 3100 K and 10 ms, respectively, when the 2D peak is the highest with f and g, indicative of the fact from the Raman spectra (Figure 21).

When the compression of the carbon source is increased between the electrodes, its conductivity increases, resulting in resistance variance of carbon source. Figure 21(e) shows the effect that the resistance of starting material of the sample has on the quality of FJH graphene.

4. Importance of Flash Joule Heating Method

Implementing the flash joule heating process to convert solid waste to flash graphene on an industrial scale has the potential to reduce the need for landfills. Compared to current solid waste treatment processes where the product is disposed of (as with ash and char from pyrolysis), flash

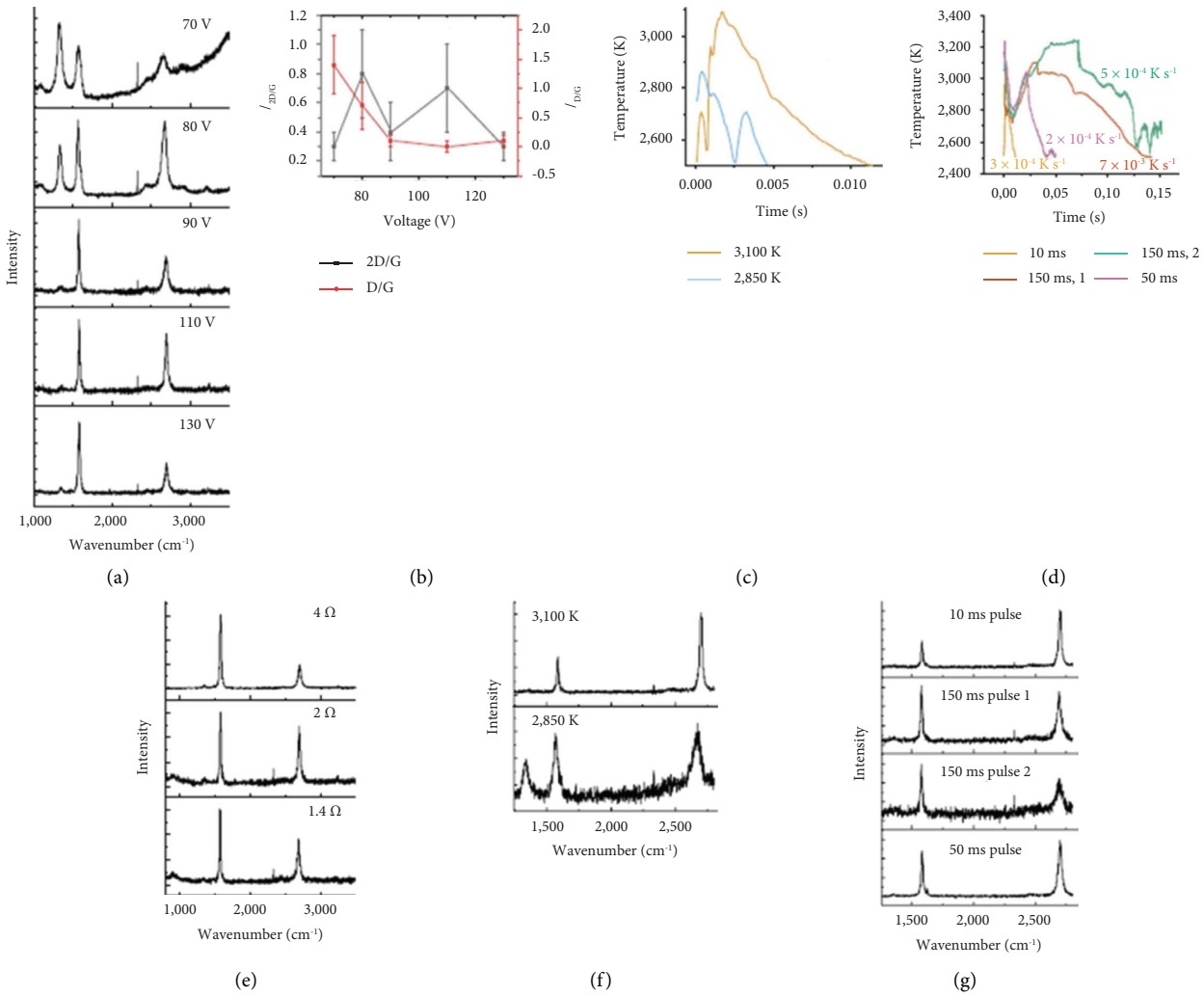

Figure 21: (a) Raman spectra of carbon black after being processed using FJH at the different initial voltage at which the capacitor bank is discharged. (b) Ratio of 2D and D peaks to G peak. Ideally, FJH graphene should have low D/G ratio (shows low defect concentration) and high 2D/G ratio (indicates turbostratic stacking). (c and f) Temperature vs time graph of FJH graphene production with Raman spectra. (d and g) Temperature vs flash duration with cooling rates and the Raman spectrum of the resulting graphene. (e) Raman spectra of FJH graphene obtained from carbon black under varying compressions [76, 77].

graphene from solid waste can be used in the construction of concrete buildings and strengthening composites. Carbon residue from gasification and pyrolysis can also be subjected to flash joule heating (refer to Table 4). The FJH process may also help with managing hazardous biomedical waste and replace existing methods of treatment, such as biochemical conversion, which are time intensive and requires a large ecological footprint, or incineration, which results in the production of carcinogenic compounds and cause pollution. Similarly, agricultural waste and used plastics can be upcycled into flash graphene without the need for the prewashing process [83]. Urban mining and removal of heavy metals from electronic waste have also been achieved using the flash joule heating process [84].

The FJH process can also be used to produce alternate fluorinated carbon phases (fluorinated amorphous carbon, fluorinated graphene, fluorinated nanodiamonds, and fluorinated concentric carbon moieties) [85] as well as 2D transition metals dichalcogenides, MoS_2, and WS_2, which have application in solar cells, transistors, photocatalysts, and spintronics [86].

5. Environmental Concerns due to Graphene Synthesis

Mass-produced graphene dispersions are commonly produced via chemical exfoliation, either using Hummer's method or a modification of it since it is cost-effective for bulk graphene synthesis [90]. However, the process requires the use of harsh ecotoxic oxidants and acids. The use of these acids and oxidants for graphite oxidizing makes wastewater treatment a challenge [91].

When comparing water consumption between oxidation-reduction exfoliation and ultrasonic exfoliation, chemical reduction uses approximately 170% more water with 70% of water use coming from H_2SO_4 production and

Table 4: Summary of flash joule heating parameters for high-quality turbostratic graphene [76, 77, 87–89].

Starting material		Starting material preparation	Mass (grams)	Resistance (Ω)	Atmospheric condition	Capacitance (mF)	Pretreatment	Final discharge voltage (VDC)	Pulse duration (ms)
Carbon black		—	0.03	1.5		60	N/A	110	50
Rubber tire		Rubber tire is shredded and mixed with carbon black (95% and 5%, respectively)	0.5	Less than one hundred	Atmospheric pressure or in a slight vacuum (10 mm Hg)	60	—	140–150	500
		Tire is pyrolyzed to produce carbon black		—					
Plastic	Polypropylene	Pyrolysis at 450°C	0.4	15		60	The pyrolysis ash is subjected to 50 V, 70 V and 90 V for 450 ms each	160	450
	Mixture of plastic waste	Plastic waste is grinded and mixed with 5% carbon black	0.1	1		60	The plastic waste mixture is subjected to 120 VAC, 60 Hz for 8 seconds in a vacuum desiccator	110	500

14% needed for cleaning the reduced graphene oxide for total usage of approximately 13000 liters per kilogram of graphene. The major water consuming processes in the ultrasonic exfoliation are the production of ethylene (57%) and diethyl ether (41%) for total usage of approximately 4800 liters per kilogram of graphene [92].

Furthermore, the ecotoxic potential of the two wet exfoliation synthesis methods is similar. The total ecotoxic potential in chemical reduction is 1.7 CTU_e/kg with the major contributor being vanadium emissions when hydrazine is produced (95%). The ultrasonic exfoliation has a total of 1.9 CTU_e/kg with ethylene production being the major contributor because of copper constituent emissions (74%) [92].

Moreover, certain oxidation-reduction exfoliation methods produce hazardous gases, namely, dinitrogen tetroxide and nitrogen dioxide [93, 94]. Also, there is a production of explosive gases, namely, acid fog and chlorine dioxide due to the use of nitric acid [95]. Additionally, the use of toxic chemicals such as aluminium hydride, hydrazine, and borohydrides as reducing agents indicates that cost and safety considerations must be accounted for when moving toward industrial-scale synthesis using wet exfoliation techniques [33].

Obtaining graphite for top-down synthesis methods adds to environmental devastation. Graphite extraction requires large-scale milling, crushing, and flotation to segregate flakes from rocks. The graphite flakes are then subjected to acid leaching to remove minerals lodged in the layers. For graphite required for battery-grade anodes, it is further processed using hydrofluoric acid and sodium hydroxide. The culmination of acid leaching and processing graphite for battery-grade anodes involves chemicals that are harmful to the environment [96].

Bottom-up synthesis methods, on the other hand, require greater energy input to enable the synthesis of graphene from various carbon precursors. While the chemical and thermal reduction methods consume approximately 0.008 and 0.0011 MJ per gram, chemical vapour deposition requires approximately 257 MJ per gram. CVD has also been studied to be the most environmentally impactful method of synthesis at a commercial scale compared to chemical and thermal reduction methods. When CVD is compared to the chemical reduction of oxidized graphite, CVD has [97]

(i) 7×10^6% greater global warming potential.

(ii) 5.5×10^6% greater photochemical ozone formation.

(iii) 35.2×10^6% greater ecotoxicity potential.

As with CVD, epitaxial growth of graphene on SiC substrate requires a copious amount of energy. While CVD energy requirements range from 7 kJ/cm^2 to 160 kJ/cm^2, epitaxial graphene requires a minimum of 2 MJ/cm^2 [98]. Additionally, certain modified versions of epitaxial growth, such as an exothermic reaction of PTFE with SiC for high-quality graphene with an oxygen content of less than 1 wt.% has environmental concerns regarding gases produced from the reaction, specifically tetrafluoro ethylene [99].

6. Conclusions

The challenges in the mass production of graphene hinder the implementation of its physicochemical properties in various applications. Chemical vapor deposition, liquid-phase exfoliation, and chemical exfoliation have shown potential for large-scale production, however, the time intensiveness, environmental risks, and inconsistency in the final products need to be overcome to successfully commercialize graphene and graphene-based products.

Regarding flash graphene, the FJH process presents a graphene synthesis route that is faster than other synthesis methods as well as economically lucrative for upscaling. Focusing research on optimizing the process parameters for obtaining flash graphene from various carbonaceous materials and reliably upscaling FJH increases the potential environmental benefits with the use of waste plastics, wood, and oil as starting materials.

Furthermore, as discussed, the environmental cost must be carefully analyzed and then remedies should be presented and applied to conserve the environment. Therefore, this review paper will be summarizing the detailed approach of graphene extraction techniques, recent advances in technologies, and the environmental cost.

Conflicts of Interest

The authors declare that they have no conflict of interest.

Acknowledgments

The authors would like to express their sincere gratitude to the authors of all the papers listed in this review paper for their timeless effort in publishing their original work. In addition, the authors appreciate these authors for using their figures in this review paper.

References

[1] L. Lin, H. Peng, and Z. Liu, "Synthesis challenges for graphene industry," *Nature Materials*, vol. 18, no. 6, pp. 520–524, 2019.

[2] J. M. Lee, H. Y. Jeong, and W. I. Park, "Large-scale synthesis of graphene films by joule-heating-induced chemical vapor deposition," *Journal of Electronic Materials*, vol. 39, no. 10, pp. 2190–2195, 2010.

[3] H. Wang, H. Wang, S. Zhang et al., "Carbothermal shock enabled facile and fast growth of carbon nanotubes in a second," *Nano Research*, vol. 15, no. 3, pp. 2576–2581, 2022.

[4] Y. Yao, Z. Huang, P. Xie et al., "Carbothermal shock synthesis of high-entropy-alloy nanoparticles," *Science*, vol. 359, no. 6383, pp. 1489–1494, 2018.

[5] K. S. Novoselov, D. Jiang, F. Schedin et al., "Two-dimensional atomic crystals," *Proceedings of the National Academy of Sciences*, vol. 102, no. 30, Article ID 10451, 2005.

[6] Y. Huang, E. Sutter, N. N. Shi et al., "Reliable exfoliation of large-area high-quality flakes of graphene and other two-dimensional materials," *ACS Nano*, vol. 9, no. 11, Article ID 10612, 2015.

[7] S. Park and R. S. Ruoff, "Chemical methods for the production of graphenes," *Nature Nanotechnology*, vol. 4, pp. 217–224, 2009.

[8] O. P. Penkov, *Tribology of Graphene*, Elsevier, Amsterdam, The Netherlands, 2020.
[9] V. Singh, D. Joung, L. Zhai, S. Das, S. I. Khondaker, and S. Seal, "Graphene based materials: past, present and future," *Progress in Materials Science*, vol. 56, no. 8, pp. 1178–1271, 2011.
[10] V. Agarwal and P. B. Zetterlund, "Strategies for reduction of graphene oxide – a comprehensive review," *Chemical Engineering Journal*, vol. 405, Article ID 127018, 2021.
[11] R. Ye and J. M. Tour, "Graphene at fifteen," *ACS Nano*, vol. 13, no. 10, Article ID 10872, 2019.
[12] K. I. Bolotin, K. J. Sikes, Z. Jiang et al., "Ultrahigh electron mobility in suspended graphene," *Solid State Communications*, vol. 146, no. 9-10, pp. 351–355, 2008.
[13] C. Lee, X. Wei, J. W. Kysar, and J. Hone, "Measurement of the elastic properties and intrinsic strength of monolayer graphene," *Science*, vol. 321, no. 5887, pp. 385–388, 2008.
[14] S. Ghosh, I. Calizo, D. Teweldebrhan et al., "Extremely high thermal conductivity of graphene: prospects for thermal management applications in nanoelectronic circuits," *Applied Physics Letters*, vol. 92, no. 15, Article ID 151911, 2008.
[15] R. R. Nair, P. Blake, A. N. Grigorenko et al., "Fine structure constant defines visual transparency of graphene," *Science*, vol. 320, no. 5881, p. 1308, 2008.
[16] W. Kong, H. Kum, S.-H. Bae et al., "Path towards graphene commercialization from lab to market," *Nature Nanotechnology*, vol. 14, no. 10, pp. 927–938, 2019.
[17] X.-Y. Wang, A. Narita, and K. Müllen, "Precision synthesis versus bulk-scale fabrication of graphenes," *Nature Reviews Chemistry*, vol. 2, no. 1, p. 100, 2017.
[18] B. Jayasena and S. Subbiah, "A novel mechanical cleavage method for synthesizing few-layer graphenes," *Nanoscale Research Letters*, vol. 6, no. 1, p. 95, 2011.
[19] J. Y. Moon, M. Kim, S. I. Kim et al., "Layer-engineered large-area exfoliation of graphene," *Science Advances*, vol. 6, no. 44, Article ID eabc6601, 2020.
[20] A. Ciesielski and P. Samorì, "Graphene via sonication assisted liquid-phase exfoliation," *Chemical Society Reviews*, vol. 43, no. 1, pp. 381–398, 2014.
[21] C. E. Brennen, *Cavitation and Bubble Dynamics*, Cambridge University Press, Cambridge, UK, 2014.
[22] E. B. Flint and K. S. Suslick, "The temperature of cavitation," *Science*, vol. 253, no. 5026, pp. 1397–1399, 1991.
[23] Y. Xu, H. Cao, Y. Xue, B. Li, and W. Cai, "Liquid-phase exfoliation of graphene: an overview on exfoliation media, techniques, and challenges," *Nanomaterials*, vol. 8, no. 11, p. 942, 2018.
[24] D. Nuvoli, L. Valentini, V. Alzari et al., "High concentration few-layer graphene sheets obtained by liquid phase exfoliation of graphite in ionic liquid," *Journal of Materials Chemistry*, vol. 21, no. 10, pp. 3428–3431, 2011.
[25] K. S. Suslick, N. C. Eddingsaas, D. J. Flannigan, S. D. Hopkins, and H. Xu, "Extreme conditions during multibubble cavitation: sonoluminescence as a spectroscopic probe," *Ultrasonics Sonochemistry*, vol. 18, no. 4, pp. 842–846, 2011.
[26] M. Yi and Z. Shen, "A review on mechanical exfoliation for the scalable production of graphene," *Journal of Materials Chemistry*, vol. 3, no. 22, Article ID 11700, 2015.
[27] K. R. Paton, E. Varrla, C. Backes et al., "Scalable production of large quantities of defect-free few-layer graphene by shear exfoliation in liquids," *Nature Materials*, vol. 13, no. 6, pp. 624–630, 2014.
[28] L. Liu, Z. Shen, M. Yi, X. Zhang, and S. Ma, "A green, rapid and size-controlled production of high-quality graphene sheets by hydrodynamic forces," *RSC Advances*, vol. 4, no. 69, Article ID 36464, 2014.
[29] J. Chen, M. Duan, and G. Chen, "Continuous mechanical exfoliation of graphene sheets via three-roll mill," *Journal of Materials Chemistry*, vol. 22, no. 37, pp. 19625–19628, 2012.
[30] S. Yang, A. G. Ricciardulli, S. Liu et al., "Ultrafast delamination of graphite into high-quality graphene using alternating currents," *Angewandte Chemie International Edition*, vol. 56, no. 23, pp. 6669–6675, 2017.
[31] T. C. Achee, W. Sun, J. T. Hope et al., "High-yield scalable graphene nanosheet production from compressed graphite using electrochemical exfoliation," *Scientific Reports*, vol. 8, no. 1, Article ID 14525, 2018.
[32] C. K. Chua and M. Pumera, "Chemical reduction of graphene oxide: a synthetic chemistry viewpoint," *Chemical Society Reviews*, vol. 43, no. 1, pp. 291–312, 2014.
[33] A. Rawal, S. H. Che Man, V. Agarwal, Y. Yao, S. C. Thickett, and P. B. Zetterlund, "Structural complexity of graphene oxide: the kirigami model," *ACS Applied Materials & Interfaces*, vol. 13, no. 15, Article ID 18255, 2021.
[34] O. Akhavan, K. Bijanzad, and A. Mirsepah, "Synthesis of graphene from natural and industrial carbonaceous wastes," *RSC Advances*, vol. 4, no. 39, Article ID 20441, 2014.
[35] X. J. Lee, B. Y. Z. Hiew, K. C. Lai et al., "Review on graphene and its derivatives: synthesis methods and potential industrial implementation," *Journal of the Taiwan Institute of Chemical Engineers*, vol. 98, pp. 163–180, 2019.
[36] S. Stankovich, D. A. Dikin, R. D. Piner et al., "Synthesis of graphene-based nanosheets via chemical reduction of exfoliated graphite oxide," *Carbon*, vol. 45, no. 7, pp. 1558–1565, 2007.
[37] Z. Fan, K. Wang, T. Wei, J. Yan, L. Song, and B. Shao, "An environmentally friendly and efficient route for the reduction of graphene oxide by aluminum powder," *Carbon*, vol. 48, no. 5, pp. 1686–1689, 2010.
[38] C. Yuwen, B. Liu, L. Zhang, S. Guo, and J. Peng, "Synthesis high-qulity graphene oxide and temperature-dependent dielectric properties of reduced graphene oxide," *Materials Research Express*, vol. 6, no. 9, Article ID 950b4, 2019.
[39] X. Mei and J. Ouyang, "Ultrasonication-assisted ultrafast reduction of graphene oxide by zinc powder at room temperature," *Carbon*, vol. 49, no. 15, pp. 5389–5397, 2011.
[40] K. Ai, Y. Liu, L. Lu, X. Cheng, and L. Huo, "A novel strategy for making soluble reduced graphene oxide sheets cheaply by adopting an endogenous reducing agent," *Journal of Materials Chemistry*, vol. 21, no. 10, pp. 3365–3370, 2011.
[41] G. G. Gebreegziabher, A. S. Asemahegne, D. W. Ayele, M. Dhakshnamoorthy, and A. Kumar, "One-step synthesis and characterization of reduced graphene oxide using chemical exfoliation method," *Materials Today Chemistry*, vol. 12, pp. 233–239, 2019.
[42] L. G. Guex, B. Sacchi, K. F. Peuvot et al., "Experimental review: chemical reduction of graphene oxide (GO) to reduced graphene oxide (RGO) by aqueous chemistry," *Nanoscale*, vol. 9, no. 27, pp. 9562–9571, 2017.
[43] R. Trusovas, K. Ratautas, G. Račiukaitis et al., "Reduction of graphite oxide to graphene with laser irradiation," *Carbon*, vol. 52, pp. 574–582, 2013.
[44] F. Alotaibi, T. T. Tung, M. J. Nine et al., "Scanning atmospheric plasma for ultrafast reduction of graphene oxide and

fabrication of highly conductive graphene films and patterns," *Carbon*, vol. 127, pp. 113–121, 2018.

[45] B. Xue, Y. Zou, and Y. Yang, "A UV-light induced photochemical method for graphene oxide reduction," *Journal of Materials Science*, vol. 52, no. 21, Article ID 12742, 2017.

[46] T. Wu, S. Liu, Y. Luo, W. Lu, L. Wang, and X. Sun, "Surface plasmon resonance-induced visible light photocatalytic reduction of graphene oxide: using Ag nanoparticles as a plasmonic photocatalyst," *Nanoscale*, vol. 3, no. 5, pp. 2142–2144, 2011.

[47] I. Jung, D. A. Field, N. J. Clark et al., "Reduction kinetics of graphene oxide determined by electrical transport measurements and temperature programmed desorption," *Journal of Physical Chemistry C*, vol. 113, no. 43, Article ID 18480, 2009.

[48] Z. Yang, Y. Sun, F. Ma, Y. Lu, and T. Zhao, "Pyrolysis mechanisms of graphene oxide revealed by ReaxFF molecular dynamics simulation," *Applied Surface Science*, vol. 509, Article ID 145247, 2020.

[49] V. v Chaban and O. v Prezhdo, "Microwave reduction of graphene oxide rationalized by reactive molecular dynamics," *Nanoscale*, vol. 9, no. 11, pp. 4024–4033, 2017.

[50] Y. Zhou, Q. Bao, L. A. L. Tang, Y. Zhong, and K. P. Loh, "Hydrothermal dehydration for the "green" reduction of exfoliated graphene oxide to graphene and demonstration of tunable optical limiting properties," *Chemistry of Materials*, vol. 21, no. 13, pp. 2950–2956, 2009.

[51] M. Gao, Y. Xu, X. Wang, Y. Sang, and S. Wang, "Analysis of electrochemical reduction process of graphene oxide and its electrochemical behavior," *Electroanalysis*, vol. 28, no. 6, pp. 1377–1382, 2016.

[52] Y. Shang, D. Zhang, Y. Liu, and Y. Liu, "Simultaneous synthesis of diverse graphene via electrochemical reduction of graphene oxide," *Journal of Applied Electrochemistry*, vol. 45, no. 5, pp. 453–462, 2015.

[53] N. Arora and N. N. Sharma, "arc discharge synthesis of carbon nanotubes: comprehensive review," *Diamond and Related Materials*, vol. 50, pp. 135–150, 2014.

[54] Y. Wu, B. Wang, Y. Ma et al., "Efficient and large-scale synthesis of few-layered graphene using an arc-discharge method and conductivity studies of the resulting films," *Nano Research*, vol. 3, no. 9, pp. 661–669, 2010.

[55] X. Fang, A. Shashurin, and M. Keidar, "Role of substrate temperature at graphene synthesis in an arc discharge," *Journal of Applied Physics*, vol. 118, no. 10, Article ID 103304, 2015.

[56] Y. M. Lin, C. Dimitrakopoulos, K. A. Jenkins et al., "100-GHz transistors from wafer-scale epitaxial graphene," *Science*, vol. 327, no. 5966, p. 662, 2010.

[57] W. Norimatsu, T. Terasawa, K. Matsuda, J. Bao, and M. Kusunoki, "Features and prospects for epitaxial graphene on SiC," in *Handbook of Graphene Set*, pp. 153–199, John Wiley & Sons, Hoboken, NJ, USA, 2019.

[58] L. Sun, G. Yuan, L. Gao et al., "Chemical vapour deposition," *Nature Reviews Methods Primers*, vol. 1, p. 5, 2021.

[59] J. H. Warner, F. Schäffel, A. Bachmatiuk, and M. H. Rümmeli, "Chapter 4 - methods for obtaining graphene," in *Graphene*, J. H. Warner, F. Schäffel, A. Bachmatiuk, and M. H. Rümmeli, Eds., pp. 129–228, Elsevier, Amsterdam, The Netherlands, 2013.

[60] O. v Penkov, "Chapter 1 - introduction to graphene," in *Tribology of Graphene*, O. v Penkov, Ed., pp. 1–10, Elsevier, Amsterdam, The Netherlands, 2020.

[61] H. Döscher, T. Schmaltz, C. Neef, A. Thielmann, and T. Reiss, "Graphene roadmap briefs (No. 2): industrialization status and prospects 2020," *2D Materials*, vol. 8, no. 2, Article ID 22005, 2021.

[62] Y. Panecatl Bernal, J. Alvarado, F. J. Rodríguez-Macias et al., "Efficient anchoring of nanostructured cadmium selenide on different kinds of carbon nanotubes," *Nanotechnology*, vol. 31, no. 27, Article ID 275601, 2020.

[63] D. v Kosynkin, A. L. Higginbotham, A. Sinitskii et al., "Longitudinal unzipping of carbon nanotubes to form graphene nanoribbons," *Nature*, vol. 458, no. 7240, pp. 872–876, 2009.

[64] I. Janowska, O. Ersen, T. Jacob et al., "Catalytic unzipping of carbon nanotubes to few-layer graphene sheets under microwaves irradiation," *Applied Catalysis A: General*, vol. 371, no. 1-2, pp. 22–30, 2009.

[65] K. Kim, A. Sussman, and A. Zettl, "Graphene nanoribbons obtained by electrically unwrapping carbon nanotubes," *ACS Nano*, vol. 4, no. 3, pp. 1362–1366, 2010.

[66] L. Xie, L. Jiao, and H. Dai, "Selective etching of graphene edges by hydrogen plasma," *Journal of the American Chemical Society*, vol. 132, no. 42, Article ID 14751, 2010.

[67] M. Terrones, A. R. Botello-Méndez, J. Campos-Delgado et al., "Graphene and graphite nanoribbons: morphology, properties, synthesis, defects and applications," *Nano Today*, vol. 5, no. 4, pp. 351–372, 2010.

[68] R. Ye, D. K. James, and J. M. Tour, "Laser-induced graphene," *Accounts of Chemical Research*, vol. 51, no. 7, pp. 1609–1620, 2018.

[69] Y. Bleu, F. Bourquard, J.-Y. Michalon et al., "Transfer-free graphene synthesis by nickel catalyst dewetting using rapid thermal annealing," *Applied Surface Science*, vol. 555, Article ID 149492, 2021.

[70] A. Dato, V. Radmilovic, Z. Lee, J. Phillips, and M. Frenklach, "Substrate-free gas-phase synthesis of graphene sheets," *Nano Letters*, vol. 8, no. 7, pp. 2012–2016, 2008.

[71] A. Dato and M. Frenklach, "Substrate-free microwave synthesis of graphene: experimental conditions and hydrocarbon precursors," *New Journal of Physics*, vol. 12, Article ID 125013, 2010.

[72] C. Melero, R. Rincón, J. Muñoz et al., "Scalable graphene production from ethanol decomposition by microwave argon plasma torch," *Plasma Physics and Controlled Fusion*, vol. 60, no. 1, Article ID 14009, 2017.

[73] E. Tatarova, A. Dias, J. Henriques et al., "Microwave plasmas applied for the synthesis of free standing graphene sheets," *Journal of Physics D: Applied Physics*, vol. 47, no. 38, Article ID 385501, 2014.

[74] D. Tsyganov, N. Bundaleska, E. Tatarova et al., "On the plasma-based growth of 'flowing' graphene sheets at atmospheric pressure conditions," *Plasma Sources Science and Technology*, vol. 25, no. 1, Article ID 015013, 2015.

[75] A. Dato, "Graphene synthesized in atmospheric plasmas—a review," *Journal of Materials Research*, vol. 34, no. 1, pp. 214–230, 2019.

[76] D. X. Luong, K. v Bets, W. A. Algozeeb et al., "Gram-scale bottom-up flash graphene synthesis," *Nature*, vol. 577, no. 7792, pp. 647–651, 2020.

[77] M. G. Stanford, K. v Bets, D. X. Luong et al., "Flash graphene morphologies," *ACS Nano*, vol. 14, no. 10, pp. 13691–13699, 2020.

[78] M. Yi and Z. Shen, "Kitchen blender for producing high-quality few-layer graphene," *Carbon*, vol. 78, pp. 622–626, 2014.

[79] W. Ren and H.-M. Cheng, "The global growth of graphene," *Nature Nanotechnology*, vol. 9, no. 10, pp. 726–730, 2014.

[80] X. Wu, Y. Liu, H. Yang, and Z. Shi, "Large-scale synthesis of high-quality graphene sheets by an improved alternating current arc-discharge method," *RSC Advances*, vol. 6, no. 95, Article ID 93119, 2016.

[81] J. Robinson, X. Weng, K. Trumbull et al., "Nucleation of epitaxial graphene on SiC(0001)," *ACS Nano*, vol. 4, no. 1, pp. 153–158, 2010.
[82] J. R. Prekodravac, D. P. Kepić, J. C. Colmenares, D. A. Giannakoudakis, and S. P. Jovanović, "A comprehensive review on selected graphene synthesis methods: from electrochemical exfoliation through rapid thermal annealing towards biomass pyrolysis," *Journal of Materials Chemistry C*, vol. 9, no. 21, pp. 6722–6748, 2021.
[83] N. H. Barbhuiya, A. Kumar, A. Singh et al., "The future of flash graphene for the sustainable management of solid waste," *ACS Nano*, vol. 15, no. 10, Article ID 15461, 2021.
[84] B. Deng, D. X. Luong, Z. Wang, C. Kittrell, E. A. McHugh, and J. M. Tour, "Urban mining by flash joule heating," *Nature Communications*, vol. 12, no. 1, p. 5794, 2021.
[85] W. Chen, J. T. Li, Z. Wang et al., "Ultrafast and controllable phase evolution by flash joule heating," *ACS Nano*, vol. 15, no. 7, Article ID 11158, 2021.
[86] W. Chen, Z. Wang, K. v Bets et al., "Millisecond conversion of metastable 2D materials by flash joule heating," *ACS Nano*, vol. 15, no. 1, pp. 1282–1290, 2021.
[87] P. A. Advincula, D. X. Luong, W. Chen, S. Raghuraman, R. Shahsavari, and J. M. Tour, "Flash graphene from rubber waste," *Carbon*, vol. 178, pp. 649–656, 2021.
[88] K. M. Wyss, J. L. Beckham, W. Chen et al., "Converting plastic waste pyrolysis ash into flash graphene," *Carbon*, vol. 174, pp. 430–438, 2021.
[89] W. A. Algozeeb, P. E. Savas, D. X. Luong et al., "Flash graphene from plastic waste," *ACS Nano*, vol. 14, no. 11, Article ID 15595, 2020.
[90] W. S. Hummers and R. E. Offeman, "Preparation of graphitic oxide," *Journal of the American Chemical Society*, vol. 80, no. 6, p. 1339, 1958.
[91] S. T. Hossain and R. Wang, "Electrochemical exfoliation of graphite: effect of temperature and hydrogen peroxide addition," *Electrochimica Acta*, vol. 216, pp. 253–260, 2016.
[92] R. Arvidsson, D. Kushnir, B. A. Sandén, and S. Molander, "Prospective life cycle assessment of graphene production by ultrasonication and chemical reduction," *Environmental Science and Technology*, vol. 48, no. 8, pp. 4529–4536, 2014.
[93] H. Yu, B. Zhang, C. Bulin, R. Li, and R. Xing, "High-efficient synthesis of graphene oxide based on improved Hummers method," *Scientific Reports*, vol. 6, no. 1, Article ID 36143, 2016.
[94] T. Somanathan, K. Prasad, K. Ostrikov, A. Saravanan, V. Krishna, and V. M. Krishna, "Graphene oxide synthesis from agro waste," *Nanomaterials*, vol. 5, no. 2, pp. 826–834, 2015.
[95] J. Chen, B. Yao, C. Li, and G. Shi, "An improved Hummers method for eco-friendly synthesis of graphene oxide," *Carbon*, vol. 64, pp. 225–229, 2013.
[96] N. A. Banek, D. T. Abele, K. R. McKenzie, and M. J. Wagner, "Sustainable conversion of lignocellulose to high-purity, highly crystalline flake potato graphite," *ACS Sustainable Chemistry & Engineering*, vol. 6, no. 10, Article ID 13199, 2018.
[97] M. Cossutta, J. McKechnie, and S. J. Pickering, "A comparative LCA of different graphene production routes," *Green Chemistry*, vol. 19, no. 24, pp. 5874–5884, 2017.
[98] R. Arvidsson and S. Molander, "Prospective life cycle assessment of epitaxial graphene production at different manufacturing scales and maturity," *Journal of Industrial Ecology*, vol. 21, no. 5, pp. 1153–1164, 2017.
[99] K. v Manukyan, S. Rouvimov, E. E. Wolf, and A. S. Mukasyan, "Combustion synthesis of graphene materials," *Carbon*, vol. 62, pp. 302–311, 2013.